Metal-Alkali Catalytic Valorization of Lignocellulose Towards Aromatics and Small Molecular Alcohols and Acids in a Holistic Approach

Wei Lv
Guangzhou Institute of Energy Conversion
Yuting Zhu
Guangzhou Institute of Energy Conversion
Weiqi Mai
South China Agricultural University
Changhui Zhu
Guangzhou Institute of Energy Conversion
Qifeng Pi
Guangzhou Institute of Energy Conversion
Chenguang Wang
Guangzhou Institute of Energy Conversion
Ying Xu
Guangzhou Institute of Energy Conversion
Qi Zhang
Guangzhou Institute of Energy Conversion
Longlong Ma (mall@ms.giec.ac.cn)
Guangzhou Institute of Energy Conversion

Research Article

Keywords: lignocellulose, catalytic depolymerization, metal-alkali, aromatics, alcohols

Posted Date: March 17th, 2021

DOI: https://doi.org/10.21203/rs.3.rs-304582/v1

Abstract

In this work, we developed an approach of one-pot completely catalytic conversion of woody biomass into two value product streams: lignin-derived aromatics (68.54% monomer and 29.65% oligomer yields of lignin) and (semi-)cellulose-derived small molecular alcohols (about 59.60% of biomass mass). These could be afforded by conducting lignocellulose depolymerization over metal-alkaline catalysts in a mixture n-butanol/H_2O solvent system at 250 °C and 30 bar H_2. In the valorization process, the homogenous mixture of n-butanol-H_2O solvents extract and depolymerize both lignin and hemicellulose, while the catalysts and H_2 are essential to cleave the inter-/intramolecular linkages of lignocellulose into target products. After the reaction, phase separation of n-butanol and H_2O takes place when systematic temperature at room temperature, providing a mild and effective strategy to isolate lignin-derived aromatics (n-butanol phase) from small molecular alcohols/acids (aqueous phase). Ru/C and alkali catalysts are collected by filtration from n-butanol phase and H_2O phase, respectively. Meanwhile, the effect of metal-alkali coupled catalysts enables facilitating the cleavage of β-O-4 linkage of lignin and increasing the attainability of (semi-)cellulose-derived oligomers and the small molecular alcohols. This catalytic system provides a versatile valorization approach for biomass catalytic to bio-based chemicals.

Highlights

- Developed an approach of one-pot completely catalytic conversion and separation of woody biomass into two value product streams: lignin-derived aromatics (68.54% monomer and 29.65% oligomer yields of lignin) and (semi-)cellulose-derived small molecular alcohols (about 59.60% of biomass mass).
- The mixture of n-butanol/H_2O solvents provide homogenous environment for lignocellulose valorization and automatically separate aromatics from small molecular alcohols. Spend Ru/C and alkali catalysts are easily retrieved with n-butanol phase and H_2O phase.
- The effect of metal-base coupled catalysts enables facilitating the cleavage of β-O-4 linkage of lignin and increasing the attainability of (semi-)cellulose-derived oligomers and the small molecular alcohols.
- The two resulting product streams and catalyst recollection provide a versatile valorization approach for biomass catalytic to bio-based chemicals.

1. Introduction

With the increasing demand of global energy and the declining of crude oil attainability as fuel, chemicals and energy [1], the proportion of energy and chemicals provided by renewable resources (such as biomass) is gradually increasing and becoming an increasingly important resource for the sustainable production of fuels and chemicals [2-3]. Combined with people's concern and pursuit for healthier and

environmentally benign products, it has become a common trend to use natural ingredients in various products to replacement of non-renewable raw materials with renewable resources and minimization of the impact of industrial waste on the environment [4-7]. Therefore, a shift of selective producing high-value chemicals from fossil to renewable carbon resources can ease the energy crisis, open up a fine chemical industry chain and reduce CO_2 emissions [8-9].

Among diverse renewable resources, biomass resources has the advantage of being abundant, clean and cheap with huge potential of utilization, and has been set to become one of the most important energy sources in the future [10-11]. Biomass serves as a natural renewable chemical resources that can be converted to high added-value products [12-14]. For example, cellulose and hemicellulose produce high value-added liquid fuels and fine chemicals (liquid fuel oil, food additives and important intermediates such as ethanol, ethylene glycol, hydroxyl ketenes, propylene glycol, glycerol, butanediol, hexadiol, polyol, acetone alcohol, acetone, lactic acid, etc.) [11, 14-22]. Lignin, the only renewable aromatic polymer, is showing its significant utilization potential for manufacture essence/spice [23-24], synthesizing value-added chemicals (dimethyl sulfoxide, alkyl phenol and lubricating oil, etc.) [13, 25-27] , liquid fuel (aromatic/olefin/paraffin) [2, 28-29] and polymers (polycaprolactone, polyester, polyurethane, phenolic resin, matrix ink and enhanced plant oil-based polyurethane composite materials, etc.) [24, 27, 30-32].

Although biomass is being a charming resource for the preparation of bulk chemicals from sustainable biomass rather than petroleum resources, biomass utilization at present has low utilization rate of raw materials and high energy consumption. Thus, it is necessary to maximize utilization biomass for competition with fossil-based processes on the cost and environmentally [7, 33] . To address the issues and realize multi-component fully conversion of lignocellulose, it is a need for the overall biomass refining technologies with low energy requirements and high carbon (and mass) efficiency. In recent years, the one-pot method has been adopted to directly catalytic conversion of lignocellulose to afford multiple chemicals by some research teams.

Zhang et al. selectively converted biomass into two sets of small molecular compounds in water over 4% Ni-30%W_2C/AC catalyst at 235℃ and 6 MPa H_2. The lignin in biomass was converted into phenolic compounds, while the cellulose and hemicellulose components were selectively degraded to ethylene glycol (EG) and 1,2-propylene glycol (1,2-PG). Especially, 36.3% of monomer phenol yield and 76.1% of glycol yield were afforded when raw material was birch wood [34] . Wang et al. reported that corn stalk was efficiently transformed in a water with a partially oxidized commercial Ru/C catalyst under 3 MPa H_2 at 200℃. Lignin was selectively converted into cycloalkanes, while the (semi-cellulose) fractions were converted into polyols, such as sugar alcohols and diols [35] . In our previous work, $LiTaMoO_6$ combined with Ru/C were applied to catalyze the transformation of real biomass in the dilute phosphoric acid aqueous solution system at 230℃ and 6 MPa H_2. Compared to the above reports, the real biomass in this work was converted (semi-cellulose) fractions to C5-C6 gasoline alkane with a yield of 82.4%. Lignin is partially converted into monomer phenols [36]. Recently, an integrated biorefinery of lignocellulose was

reported in Science by Bert Sels' Group with 78 wt % of birch was converted into xylochemicals. Carbohydrate pulp and lignin oil were firstly separated in one-pot by reductive catalytic fractionation (RCF) of lignocellulose. After that, lignin oil was extracted to phenolic monomers for producing 20 wt% of phenol and 9 wt% of propylene (on lignin basis) by gas-phase hydroprocessing/dealkylation, and the residual phenolic oligomers (30 wt%) were used in printing ink. Whereas the carbohydrate pulp was used to produce bioethanol (40.2 g/L^{-1}) by biological fermentation [7].

Due to the great difference of lignin and (semi-cellulose) structures, the final depolymerized products derived one-pot conversion of biomass are too complex and quite different, product separation is necessary for upgrading or utilization after the end of the reaction. However, product separation is difficult to operate and will increase production costs. In other words, although one-pot catalytic hydrodeoxygenation conversion of lignocellulose to hydrocarbon fuel has a certain prospect of application, there are still some shortcomings in the preparation of high value-added chemicals. Therefore, the strategy of valorization lignocellulose into chemicals needs to be further improved.

Herein, we developed and investigated a catalytic valorization route, targeting the one-step conversion of woody biomass and separation into two sets of value products: (i) lignin derived aromatics, (ii) (semi-)cellulose-derived small molecular (C2~C5) alcohols and acids (Fig.1). In order to provide an effective depolymerization and separation approach of the solubilized fractions, metal-alkali completely catalytic depolymerization biomass was performed in biphasic n-butanol/H_2O solvent system. After the reaction, lignin-derived phenolic compounds and (semi-)cellulose-derived products were automatically extracted and separated by n-butanol phase (upper) and aqueous phase, respectively. Which is reduced the difficulty of the product separation and production cost in one-pot complete dissolution polymerization system.

2. Experimental Section

2.1 Materials

All used chemical reagents and materials in this work are shown in the supporting information.

2.2 Typical process for lignocellulose valorization

Depolymerization experiments were conducted in a 100 ml autoclave (Hastelloy alloy, made by Anhui Kemi Machinery Technology Co., Ltd.) equipped with a mechanical stirring. In a typical depolymerization reaction, 2.0 g pre-extracted powder was put into the reactor with the catalyst (0.2 g Ru/C or / and 0.4g MgO) and the n-butanol/water solvent mixture (40 mL, v/v=1:1). The reactor was sealed, replaced the air in the reactor by N_2 four times and then by H_2 three times. A total of 30 bar of H_2 was pressurized at room temperature. The reaction mixture was heated to 200 °C (~10 °C min^{-1}) and then kept for 2h with continuous stirring at 700 rpm. After that, the reactor was cooled and collected the gaseous products at room temperature.

2.3 Products separation

The liquid and solid mixtures were taken out and the reactor was washed with 15 mL water and 15 mL n-butanol. The obtained mixture was filtered to separate solid and liquid mixture. The mixture of solid (Ru/C, Mg (OH) $_2$ (MgO converts to Mg (OH) $_2$ in hydrothermal condition) and depolymerization residue) were separated and collected through liquid-liquid extraction method with n-butanol and H_2O. Ru/C primarily resides (due to its relatively polar) in n-butanol phase, while Mg (OH) $_2$ and powder residue (if any) were located at aqueous phase. After liquid-liquid extraction, portion of Ru/C was extracted in the n-butanol phase and then retrieved, the reminder Ru/C blended with $Mg(OH)_2$ and powder residue (if any) in H_2O phase was extracted again with fresh n-butanol. This was repeated until the n-butanol phase remained relatively clear. All of the collected Ru/C was washed with ethanol to remove n-butanol and other adsorbents until alcoholic filtrate relative clear. The mixed solid (powder residue and $Mg(OH)_2$)) was calcinated to retrieve MgO in air under 550℃for 4h. On the other hand, the liquid products transferred to a separating funnel and automatically separated into n-butanol phase (upper phase) and aqueous phase (bottom phase), as depicted in Fig.1. After phase separation, a 20mL fresh n-butanol was added to aqueous phase for extraction lignin-derived fragments, repeating this step three times. In this way, the total n-butanol fraction measured calculating about 80 mL and the total aqueous fraction was about 43 mL.

2.4 Determine the components of lignocellulose and residue

The bits of eucalyptus wood was smashed and sieved to the wood powder (40~60 mesh). Then the extractions were removed by a Soxhlet extractor. This wood powder, hereinafter marked as ‘pre-extracted powder’, was used for composition analysis. The composition is summarized in Table S1. The composition of eucalyptus powder and depolymerization residue were analyzed by NREL according to NREL Laboratory Analytical Procedures [37].

Eucalyptus powder and residue before and after depolymerization were characterized by XRD and FT-IR.

2.5 Analysis and measurement of gaseous and liquid products

The n-butanol phase was analyzed by GC-FID and GC-MS. Acetophenone was added as an internal standard for quantification. The aqueous phase was analyzed by HPLC. The gaseous products were analyzed by GC. The distribution of the molar weight of the lignin products was investigated using gel permeation chromatography (GPC). The structure characteristic of lignin fragments were analyzed by HSQC analysis. The detail information was provided in the supporting information.

3. Results And Discussion

3.1 Ru/C cooperated with MgO for catalytic valorization lignocellulose

Eucalyptus powder, composition summarized in Table S1, was mostly catalytic depolymerized to liquid products over the catalysts (Ru/C-MgO) in biphasic solvent (n-butanol/H_2O). The eucalyptus valorization process is displayed in Fig.1. Here, 2.0 g pre-extracted eucalyptus powder, 0.2 g of Ru/C and 0.4 g MgO catalysts, and 20 mL H_2O, 20 mL n-butanol were put in a 100 mL autoclave equipped with a mechanical stirring. The autoclave was sealed, purified and pressurized with H_2 (30 bar), and the mixture was stirred (700 rpm) and heated to a given temperature of 250 °C for 6 h. After cooling to room temperature, the gaseous and liquid fractions were collected and processed. The solids (pretty much were Ru/C and Mg $(OH)_2$) were washed with refresh H_2O and n-butanol. The filtrate instantly separated into n-butanol (containing lignin-derived products) and aqueous phase (including (semi)cellulose-derived products) (Fig.1). Thereby providing an effective depolymerization and separation of the soluble products (Scheme S1, supporting information for experimental and separated procedures). Evaporation of n-butanol yielded a viscous oil with 23.85 wt % of the initial biomass weight. The weight of the n-butanol oil is close to the total lignin content of the eucalyptus sawdust (25.97 wt %), indicating extensive lignin extraction from the biomass.

The lignin oil in n-butanol phase contains a large number of aromatic monomers, corresponding to a yield of 68.54 wt % based on total lignin content of the eucalyptus powder. The monomer aromatics mainly include propanol-substituted syringol/guaiacyl ((label as S_3-OH/G_3-OH), propyl-substituted syringol/guaiacyl ((label as S_3 /G_3), methyl-substituted syringol/guaiacyl (S_1/G_1), and a small amount of 2,6-dimethoxyphenol/guaiacol ((label as S_0/G_0) and ethyl-substituted syringol/guaiacyl ((label as S_2/G_2) (Fig. 2A). Compared to the monomer aromatics (S_3-OH/G_3-OH, S_3 /G_3 and S_2/G_2) derived from Ru/C catalyzed depolymerization eucalyptus in n-butanol/H_2O solvents [38-39], another 14.32 wt % of S_0/G_0 and S_2/G_2 monomer aromatics (on lignin oil basis) are obtained, which is ascribed to the presence of MgO. The molecular weight distribution of the lignin-derived non-volatiles products in the n-butanol phase was investigated by GPC analysis. The result in Fig. 2C displays that n-butanol phase consists of monomers, dimers, trimmers and oligomers. The D_p (from 14~17.5 min) of oligomers is 1.25. The largest oligomers elute at 15 min, which corresponds to about a M_w of 1600 g mol^{-1}. The result of HSQC NMR indicates that the lignin inter-unit ether bonds almost disappear (Fig. 2E), and no lignin typical absorbance peak in FT-IR of residual further evidence the absence of lignin in residue (Fig. 2D). Hence, we infer that lignin is degraded effectively over Ru/C-MgO catalysts in the biphasic n-butanol/water solvents system.

Products in the aqueous phase were analyzed by GC-MS and quantified with HPLC (Fig. 2B). Products comprise acetic acid (29.65 $mg{\cdot}g_{biomass}^{-1}$), EG (96.85 $mg{\cdot}g_{biomass}^{-1}$), 1,2-PG (88.78 $mg{\cdot}g_{biomass}^{-1}$), ethanol (79.61 $mg{\cdot}g_{biomass}^{-1}$), 1-hydroxy-2-butanone (69.46 $mg{\cdot}g_{biomass}^{-1}$), tetrahydrofurfuryl alcohol (94.03 $mg{\cdot}g_{biomass}^{-1}$) and oligomers (22.2 $mg{\cdot}g_{biomass}^{-1}$), a little C5~C6 polyol fractions (glucose, sorbitol and xylitol). FT-IR (Fig. 2D) result shows the cellulose and hemicellulose were almost converted since no typical peak was observed. Therefore, we conclude that cellulose and hemicellulose pretty much depolymerized effectively to small molecular alcohols/ acids over Ru/C-MgO catalysts in this system. Additionally, except for cellobiose, the other oligomer fractions are hard to qualitatively analyze (Fig. S9-

6h) and the mass of oligomer was calculated via Eq. (9) in supporting information. Besides H_2, very few other gaseous generated and the mass was not calculated (Table S2). A general mass flowchart of the main lignocellulose constituents is presented in Fig.3.

The fractions from liquid and solid phases (not included gas phase due to a little amount of gas), in relation to the composition of the eucalyptus (Table S1). All numbers are expressed as wt % relative to the mass of eucalyptus powder. Compared to Fig.2A and 2B, acetic acid, EG and 1,2-PG in n-butanol phase were calculated into n-butanol phase products in Fig.3, similarly, the monomer aromatics in aqueous phase were calculated in aqueous phase products in Fig.3. Reaction conditions: 20 mL n-butanol, 20 mL water, 2 g extracted eucalyptus powder, 0.2 g Ru/C and 0.4g MgO catalysts, 30 bar H_2, 250 °C, 6 h.

3.2 Effect of solvent on lignocellulose valorization

To illuminate the necessity of biphasic solvents, valorization of eucalyptus with Ru/C or/and MgO was performed in pure n-butanol and pure water. After reaction, a similar products separation procedure (supporting information) was conducted for products qualitative and quantitative analysis.

When eucalyptus powder was depolymerized in pure n-butanol solvent system over Ru/C, MgO and Ru/C-MgO catalysts, lignin oil yield was 9.13 wt %, 10.28wt % and 13.65 wt %, respectively. Apparently, pure n-butanol has poor effective for the depolymerization process, which is also reflected by the low lignin monomer yield (10.1 wt %, 20.2wt % and 23.6 wt %, respectively, on lignin basis, Fig.4A). Additionally, barely aqueous phase products in the aqueous phase (Fig.4B and Fig.S3B) also confirmed n-butanol has very poor effect on the cleavage of linkage in cellulose and hemicellulose.

Compared to depolymerizing in pure n-butanol system, the valorization process in pure water system provides higher aromatic monomer yield. For instance, the monomer yield was increased to 28.56 wt% and 26.05 wt% in Ru/C and Ru/C-MgO cases, respectively (on lignin basis, Fig.4A). Despite this, product yields are lower than that of in biphasic solvent system cases, confirming by weaker peak intensity response of GPC curves (Fig.S1). The obvious difference that the structure of lignin depolymerization products changed in pure water system. The products are cyclohexanol derivatives A to F (Fig. 4A) due to the hydrogenation of benzene ring and disproportionation of side chain alkyl group [7, 40]. The hydrogenation of benzene ring probably ascribed to the sorption behavior of phenols on the catalyst surface that are affected by water. Bert Sels and co-workers also considered that the phenolic incompatibility with water leads to phenols adsorb on the catalyst surface and facilitate benzene ring hydrogenation [39, 41-42]. In contrast, in the presence of alcohols, as well as Ru/C catalyst, phenolic compounds are easier to dissolve in alcohols and protected by the alcohol solvent from being subjected to ring hydrogenation and subsequent demethoxylation [39, 41] . The products from the valorization process in n-butanol/H_2O also confirm this conclusion (Fig. 4A), i.e. benzene ring and side-chain methoxy group are reserved in n-butanol/H_2O.

Apparently, the biphasic n-butanol/H_2O provided higher lignin oil and monomer aromatic yields compared to either pure n-butanol or pure H_2O, which is consistent with deopolymerizatin lignin in ethyl acetate/H_2O [43-44], methanol-H_2O [45-46] and ethanol-H_2O [44, 46]. On the other hand, the molecular weight of aqueous phase product is lower for the reaction in water than in biphasic solvent system (Fig. 4B). This results is ascribed to the polarity of n-butanol-H_2O is lower than that of pure H_2O (n-butanol/water mixture is monophasic when the temperature is above 125℃(n-butanol/H_2O upper critical solution temperature)) [47-48], which prevents the oligomers further degrading in hydrolysis process, and was also evidenced by more oligomers in aqueous phase (HPLC, Fig. S3A and Fig. S3C). However, it cannot be ignored that butanol/ H_2O has a dual behavior [39]. When the temperature is higher than 125℃, they becomes a homogeneous system (homogeneous phase solvent system is considered more appropriate for depolymerization [49-51]), which avoids the inherent complexity of the biphasic phase solvent system. When the temperature is lower than 125℃ like after the reaction, the solvent system gets back to two phases for product separation. Therefore, n-butanol/H_2O mixture is homogeneous phase under valorization temperatures (160~280℃) and more appropriate for valorization.

3.3 Effect of catalysts in n-butanol/H_2O solvent system

3.3.1 Effect of catalysts on lignin valorization

To understand the effect of the catalysts, catalytic depolymerization eucalyptus powder was performed in n-butanol/water over different catalysts（without catalyst, over MgO, Ru/C or Ru/C-MgO catalysts）. To avoid eucalyptus powder was degraded completely over all of catalysts at too high reaction temperature (it is not conducive to comparing the activity of catalysts), a relative lower temperature was chosen (200℃). Notably, liquefaction rate of eucalyptus powder (Table S3), monomer aromatic selectivity and the yield of total monomer aromatics differs dramatically (Fig.4A). Ru/C and Ru/C-MgO catalysts afford almost same biomass liquefaction rate (65.33/65.92%), conversion of lignin (91.2/92.26%) and hemicellulose (79.97 / 80.69%). While MgO provides much lower biomass liquefaction rate and lignin conversion than Ru/C and Ru/C-MgO catalysts. These results are also confirmed by FT-IR (Fig. S2).

The yield of monomer aromatics increased in the order of without catalyst＜MgO＜Ru/C＜Ru/C-MgO (Fig.4A) and the distribution of products differ dramatically. Without catalyst, the main monomers are 4-(2-Propenyl) guaiacol / 4-(2-propenyl) syringol (label as G3/S3$^=$) and 4-hydroxy-3-methoxybenzaldehyde / 4-hydroxy-3, 5-dimethoxybenzaldehyde (label as G1/S1=O). For the reaction catalyzed by MgO, the aromatic monomer yield was significantly increased to 21.2% from 8.7% (without catalyst). The yield of 4-n-propanolguaiacol / 4-n-propanolsyringol (label as G3/S3-OH) significantly increased but 4-(2-propenyl) guaiacol / 4-(2-propenyl) syringol (label as G3/S3$^=$) and G1/S1=O decreased compared to without catalyst. Meanwhile, a little amount of 3-methoxy-4-hydroxyphenylacetic acid / 3,5-dimethoxy-4-hydroxyphenylacetic acid (label as G2/S2=OOH), 2-(4-hydroxy-3-methoxyphenyl)acetaldehyde / 2-(4-hydroxy-3,5-dimethoxyphenyl) acetaldehyde (label as G2/S2=O), 2-methoxy-4-vinylphenol / 2,6-dimethoxy-4-vinylphenol (label as G2/S2$^=$) and guaiacol / syringol (label as G0/S0) appeared (Fig.4A). It

was reported that MgO can produce a hydroxo complex ($Mg(OH)_2$) under hydrothermal conditions [52], which may be related to the formation of G2/S2=OOH, G2/S2=O□G0/S0 and G2/S2$^{=}$ from lignin conversion under hydrothermal conditions [21, 53]. While only Ru/C in n-butanol/H_2O system for depolymerization, the total monomer aromatic yield is 47.15% with main products G3/S3-OH and 4-n-propylguaiacol / 4-n-propylguaiacol (label as G3/S3). G3/S3 derived from the dehydration-hydrogenation of G3/S3-OH or hydrogenolysis of G3/S3-OH. A small number of G3/S3$^{=}$ and 4-methylsyringol /4-methylguaiacol (label as G1/S1) are obviously from dehydration and decarbonylation reactions. When Ru/C combined with MgO, although about 12.6% of monomer aromatic yield is higher than that in Ru/C case, the relative selectivity of aromatics decreased. For instance, G3/S3-OH decrease to 25.90% from 32.70%, G0/S0, G1/S1, G2/S2 and G2/S2=OOH obviously increase to their total yield of 16.93% from 6.13%. These results are attributed to the synergistic effect between Ru/C and MgO catalysts on (i) converting a portion of G3/S3-OH to G3/S3$^{=}$ and subsequent converting to G0/S0 through inverse hydroxyaldehyde reaction of G3/S3$^{=}$ and decarbonylation reaction of G2/S2=O [43, 54]; (ii) enhancing the conversion of quinone methides and enol ethers to G1/S1, G2/S2 and G2/S2=OOH under basic catalysis [2, 26].

As for the non-volatile lignin oil, it can be found that just a few lignin fragments were dissolved by n-butanol/H_2O solvents (GPC, Fig.S1A), which is consistent with strong lignin characteristic absorption peaks in FT-IR of the residue (Fig. S2). Although the typical absorbance peaks of lignin in the residue significantly reduced with MgO catalyst, the lignin fragments with very large molecular weight were found to be broadly distributed in lignin oil (Fig.S1A). In the Ru/C and Ru/ C-MgO cases, a large amount of lignin fragments with M_w=155~897 were afforded after depolymerization. It indicates that both of Ru/C and Ru/C-MgO demonstrated good degradation ability to lignin in n-butanol/H_2O system. The weak lignin characteristic absorbance peaks in FT-IR of the residue (Fig. S2) are consistent with these GPC results (Fig. S1C). In addition, it can be seen from the side chain spectra of HSQC that most of the alkyl side chains were retained in non-volatile lignin oil in all cases (Fig.5). However, the cleavage of intermolecular linkages in lignin oil also strongly differ over different catalysts. Without catalyst, a large number of intermolecular linkages were observed in lignin oil, such as β-O-4 (A_γ), β-β (B_γ), α-O-4 (C_γ) and β-5 (C_γ). A portion of β-O-4 (A_γ), α-O-4 (C_γ) and a spot of β-5 (C_γ) were cleaving over MgO catalyst. Noticeably, except for part of β-O-4(A_γ) linkages was remained in lignin oil over Ru/C catalyst, the linkage of β-β (B_γ), α-O-4 (C_γ) and β-5 (C_γ) were almost broken. When Ru/C combined with MgO, the β-O-4 (A_γ) fingerprint signal was weaker than in Ru/C case (Fig.5C-D), implying the synergetic effect from Ru/C-MgO promoted the cleavage of β-O-4(A_γ) linkage□while the residual signal of β-β (B_γ) (Fig.5D) indicates the cleavage of β-β (B_γ) linkage was inhibited by the synergetic effect.

3.3.2 Effect of catalysts on (semi-) cellulose valorization

Fig.2B displays the composition and yield of the aqueous fraction in different catalyst cases. All catalysts gave aqueous fraction yields in the range of 143.16~228.04mg based on total biomass mass.

Observably, the aqueous component selectivity differs strongly. A large amount of soluble oligomer, some acetic acid, acetol, formic acid and glycerine were afforded without catalyst (Fig. 4B and Fig.S3A), implying n-butanol/H_2O have the hydrothermal effect on the cleavage of intermolecular linkage of (semi-)cellulose. Compared to without catalyst, the weight of aqueous phase products in MgO case was slightly increased, the effect of MgO lead to decrease the soluble oligomer yield and increased acetic acid, formic acid, lactic acid (LA) and glycerol yield (Fig.4B and Fig.S3A). It is attributed to the cellulose and hemicellulose are easily degraded into small molecular acids under alkaline conditions [55-58]. The alkaline catalyst (MgO) has the ability to promote lactic acid formation from monosaccharides (/glucose/fructose/erythritol/aldoses). For Mg^{2+} (MgO converts to Mg $(OH)_2$ in hydrothermal condition) coordinates to ring oxygen or hydroxyl, it may catalyze the ring-opening or C-C bond cracking reactions, resulting from the destruction of sugar ring or C-C bond structures and promoting the formation of low-molecular weight products. These types of oxygen–Mg^{2+} coordination could lower the activation energy of the reaction [57, 59-60]. Meanwhile, with the presence of $Mg(OH)_2$, lactic acid also produce from the direct decomposition of glycerin, and the decomposition of lactic acid could lead to the production of formic and acetic acids [57, 61]. Some of acetic acid and formic acid may also come from the depolymerization of lignin [43-44].

Ru/C is regard as an excellent hydrogenation catalyst for (semi-)cellulose (polysaccharides) hydrolytic degradation because of its superior activity and selectivity [62-67]. Here, 0.2g of aqueous products were afforded with little oligomer (HPLC, Fig.S3A) over Ru/C catalyst. The mainly monomers are acetic acid, formic acid, 1, 2-Propanediol (1, 2-PG), ethanol, tetrahydrofurfuryl alcohol, EG and acetol. It has been reported that sugars (glucose, fructose and erythritgose) from (semi-)cellulose can also be degraded to small molecules by retro-aldol reaction and further degraded to ethanol, tetrahydrofurfuryl alcohol and EG [68-69]. Meanwhile, acetol also afforded from the hydrogenolysis of cellulose over hydrogenation catalyst (be similar to Ru/C) [70-71].

Differently, the yield of 1-hydroxy-2-butanone and dissolved oligomer obviously increased when reaction over Ru/C combined with MgO catalysts (Fig.4B and Fig.S3A). 1-hydroxy-2-butanone may be ascribed to glucose (from cellulose hydrolysis) isomerization to fructose by alkaline catalyst, which broke C-C bond by inverse aldol reaction and subsequent cleaved C-O bonds to 1-hydroxy-2-butanone [17, 72]. The increase of oligomer yield benefited by the synergetic effect of hydrogenolysis (Ru/C) and alkaline (MgO) that promote the cleavage of the hydrogen linkages among lignin, hemicellulose, and cellulose. However, the synergistic effect between Ru/C and MgO inhibits the conversion of glucose to C5/C6 alcohols (Fig. 4B and Fig.S3A).

Thus, the synergistic effect between Ru/C and MgO catalysts promoted to cleave β-O-4 (A_γ) linkages and inhibited to break β-β (B_γ) linkages of lignin. This interaction also increased the attainability of aqueous oligomers and the small molecular alcohols (such as EG, 1, 2-PG, 1-hydroxy-2-butanone) rather than C5/C6 alcohols and sugar.

3.4 Effect of reaction conditions on eucalyptus powder depolymerization

3.4.1 Influence of hydrogen pressure & reaction network

In addition to the effect of catalyst interactions and solvents, hydrogen pressure influenced the outcome of lignocellulose valorization in biphasic n-butanol/ H_2O solvent. To investigate its influence on the catalytic depolymerization process, the process was performed under different hydrogen pressures, between 0 to 40 bar. Without external pressure (0 bar H_2), the Ru/C-MgO depolymerized process selectively generated G1/S1, G2/S2 and $G3^{=}$/$S3^{=}$ monomers (Fig. 6A). Despite the high monomer selectivity, the total monomer yield is low (about 17 wt%), indicating inefficient stabilization of reactive intermediates. This is confirmed by GPC analysis, just obtaining a small amount of relatively large molecular weight oligomers (Fig.6C). Increasing the H_2 pressure from 0 to 10 bar strongly enhances the monomer yield depending on the increase of G3/S3-OH yield. The monomers mainly comprise G3/S3 and G3/S3-OH when the H_2 pressure from 10 to 40 bar, with the selectivity of G3/S3-OH is slightly increase with increasing H_2 pressure. The monomer yield is highest when the H_2 pressure was applied under ≥30 bar. Under these conditions, G3/S3-OH, G1/S1and G2/S2 are the predominant monomers. Above 30 bar H_2, the monomer yield doesn't exhibit increase but with an slightly selectivity increase to G2/S2 and G1/S1, which is ascribed to quinone methides convert to ethyl/methyl-substituted G/S through hydrolysis and hydrogenation/decarbonylation under high H_2 pressure over alkali catalyzation. [26] Meanwhile, about 3.90% yield of homosyringic acid (3, 5-dimethoxy-4-hydroxyphenylacetic acid, S2=OOH) also obtains, it may be from aromatic aldehyde oxidation.

The trends deduced from Fig. 6A contribute to constructing the reaction network for native lignin catalytic conversion (Fig.1). Coniferyl and sinapyl alcohol were identified as key intermediates in recent publications [38, 45, 46, 38]. The unsaturated compounds ($G3/S3^{=}$ and G1/S1=O) can even generate by solvothermal effect and are unstable at elevated temperature (Scheme 1, pathway P1, P3 and P8) in absence of catalyst [45]. Coniferyl and sinapyl alcohol are the key substances in Scheme 1, they can either undergo hydrogenation of the C_α=C_β bond to propanol-substituted G/S (pathway P2); repolymerisation, producing soluble lignin oligomers (pathway P4); hydrogenolysis of the hydroxy group on C_γ to propenyl-substituted G/S (pathway P3); or retrograde aldol of propenyl-substituted G/S on the C=C bond of side chain to formoxyl-substituted G/S (pathway P8) or/and non-substituted G/S (pathway P9).

In the present of catalysts, the alkili depolymerization and hydrogenation/hydrogenolysis are combined to depolymerize lignin. On the one hand, coniferyl and sinapyl alcohol were identified as key intermediates in hydrogenation/hydrogenolysis processes. On the other hand, quinone methide (**3**) was considered as the pivotal intermediates and was yielded under alkili reaction environment (pathway M3). In absence of pressurized hydrogen, the hydrogenolysis (pathway P3, M7), hydrolysis (pathway M6), hydrogenation route (pathway M8) and decarbonylation (pathway M9 /decarboxylation (pathway M11) routes prevail, as indicated by the high selectivity towards $G3/S3^{=}$, G2/S2 and G1/S1 monomers (Fig.6A). The solvent or solubilized carbohydrates may act as reducing agent [47, 53]. However, the rather low

monomer yield obtained in absence of external H_2 also suggests the appearance of repolymerisation (pathway M5 and/or P4 and/or P7), which involves unsaturated sidechains [38, 45]. Repolymerisation can be prevented by hydrogenating these unsaturated bonds [38, 45], thereby produce stable phenolic products. Under a relatively low H_2 pressure (10 bar), hydrogenation of coniferyl/sinapyl alcohol (pathway P2) and hydrogenolysis of propanol-substituted G/S (pathway P5) are the major reaction pathways, resulting in generating G3/S3-OH and G3/S3 monomers (Fig.6A). Meanwhile, 2.21% of G3/S3$^{=}$ monomers (Fig.6A) indicates that hydrogenolysis of coniferyl/sinapyl alcohol (pathway P3) and subsequent hydrogenation of propenyl-substituted G/S (pathway P6) also constitutes the reaction pathways. With the H_2 pressure further increasing, direct hydrogenation of coniferyl / sinapyl alcohol (pathway P2) becomes predominant, thus selectively producing more G3/S3-OH monomers. Hydrogenolysis of propanol-substituted G/S (pathway P5) is not continued when the H_2 pressure increases from 20 bar to 40 bar with a very slightly change yield of G3/S3 monomers. This selectivity change can be explained by the fact that hydrogenolysis reactions are negative order in the relative high hydrogen pressure, in contrast to hydrogenation reactions [73]. Moreover, Quinone methide takes off formyl group (pathway M4) to enol ether and subsequent hydrolysis (pathway M6) or/and hydrogenolysis (pathway M7) to ethenyl / ethanoyl-substituted G/S, and then hydrogenation of ethenyl-substituted G/S to ethyl-substituted G/S (pathway M8); or decarbonylation of ethanoyl-substituted G/S to methyl-substituted G/S (pathway M9) [2, 26]. It is thereby inferred that high H_2 pressure is contributed to the increase of G2/S2 and G1/S1 monomers. It is worth noting that acetoxy-substituted G/S is detected when hydrogen pressure is higher than 30 bar, which is attributed to oxidation of ethanoyl-substituted G/S to acetoxy-substituted G/S (pathway M10), and the oxygen likely come from lignocellulose depolymerization process.

In addition, the effect of hydrogen pressure on the carbohydrate products in the aqueous phase is illustrated in Fig.6B. In absence of pressurized hydrogen, the yield of targeted carbon hydrate products is a little low than under other pressurized hydrogen, while the monomers yield is the highest. Although the mass oligomers and the component of main monomers are similar with the carbon hydrate products in MgO case under n-butanol/H_2O (Fig.4B), MgO has great effect on the selectivity of the monomer carbon hydrate products [15-17]. DMF is obtained under 0 and 10 bar pressurized hydrogen, which is ascribed to the hydrogenation and subsequent hydrogenolysis of 5-hydroxymethylfurfural (HMF) produced from catalytic dehydration of cellulose under low hydrogen pressure. Much soluble carbohydrate products increase with the mass of oligomers increasing and monomers decreasing when the hydrogen pressure increases from 10 bar to 40 bar, indicating that high H_2 pressure facilitates the cleavage of intermolecular linkages between lignin and cellulose/hemicellulose. The mass of acetic acid and methanol slightly change with the H_2 pressure increasing (Fig.6B and 6D), likely they derive from lignin depolymerization [10–12]. With increasing pressure, the mass of soluble carbohydrate products gradually increases and reaches a plateau at 30 bar. The mass of carbon hydrate oligomers follows a similar trend, as HPLC profile shown (Fig.6D). Depolymerization (i.e. hydrogenation) of the solubilized cellulose and hemicellulose thus requires a higher hydrogen pressure than lignin valorization. At relatively low hydrogen pressure, lignin valorization proceeds effectively through the hydrogenation-dehydration-hydrogenation

(pathway P2+ P3+P6, in Scheme 1). Overall, 30 bar H_2 is the optimal pressure range to acquire high yields of both aromatics and the mass of soluble carbohydrate products.

3.4.2 Effect of reaction temperature

Subsequently, we investigated the effect of reaction temperature, since it is known that temperature greatly promote hemicellulose and cellulose hydrolysis and delignification during depolymerization [39, 40, 54]. Similar experiments were therefore conducted at 160~180℃and 220~280℃. Results of this investigation are summarized in Fig.7. As shown in Fig.7A, the lignin oil and lignin monomer yield decreased with decreasing temperature, pointing out incomplete delignification at 160 and 180 ℃. However, other monomers, benzene rings are hydrogenated by surplus hydrogenation activity, suggests that low reaction temperature can cause side reactions of benzene ring hydrogenation over Ru/C catalyst. Obviously, the change of reaction temperature show less effect on the product components (G3/S3-OH, G3/S3, G2/S2=OOH, G2/S2, G1/S1 and G0/S0), while the yield of lignin oil and monomers increase with temperature increasing (Fig.7A). Both the increase of the monomers yield and G3/S3 yield indicate that oligomers were converted to G3/S3-OH and subsequent hydrogenolysis of G3/S3-OH (pathway P3) and hydrogenation of G3/S3$^{=}$ to G3/S3 (pathway P6). With temperature elevating, the yield of G3/S3-OH slightly changes, implying that oligomer converted to G3/S3-OH. Meanwhile, it is seemed that G2/S2=OOH and G2/S2 were not affected under elevated temperature, likely attribute to less influence of temperature on M8 and M10 reaction pathways. Interestingly, G1/S1 and G0/S0 derived from decarbonylation reaction of M10 and P9 pathways, respectively, their yields slightly change at 200~250℃，but G1/S1 yield increased and G0/S0 decreased obviously at 280℃，probably pathway M10 was facilitated and pathway P9 was inhibited when temperature above 250℃. The decrease of G0/S0 mainly due to the generation rate of G1/S1=O cannot match the rate of G1/S1=O decarbonylation [54], resulting in condensation of surplus G1/S1=O. This observation was also verified by GPC analysis. The chromatogram of the non-volatiles obtained from 180°C~220°C displays the increasing large peak of oligomers and a not obvious increasing of monomer yields with the temperature increasing. Low yield of lignin oil and aromatic monomers at 160°C in agreement with the small peak of non-volatiles in chromatogram. The slightly increase of aromatic monomer and lignin oil yield are ascribed to the decrease of oligomers when the temperature above 250°C (Fig. S6).

Moreover, temperature shows great effect on hemicellulose and cellulose degradation process. For instance, below 200 ℃，just some hemicellulose degraded to form soluble oligomers. A rapid increase of carbohydrate product mass to 230 mg with 40 mg of 1-hydroxy-2-butanone at 200℃ (Fig.7B). The typical XRD diffraction peak of cellulose (2θ=15.2°(1-10), 22.8° (200), 34.5°(004)) in residue is weakening from 160~250℃ and disappearing when eucalyptus powder was depolymerized at 280℃(Fig.S5). From XRD analysis of depolymerization residue, the diffraction peaks at 15.2°(1-10) and 34.5°(004) were completely removed from cellulose matrix to dissolve in aqueous phase at 220℃, while the diffraction peak at 22.8° (200) disappeared above 250℃.The increasing temperature leads to an increased dissolution of hemicellulose and cellulose, from 7.1wt% up to 100 wt%. Accordingly, a large amount of

solubilization oligomers converted to small molecular products with the temperature increasing (Fig.7B). The mass of oligomers gradually increases with increasing temperature (Fig.7B), from 41mg•$g_{biomass}^{-1}$ to 250 mg•$g_{biomass}^{-1}$. The mass of acetic acid changes slightly, being similar with the trend in different H_2 pressure cases (similar mass of 55 mg•gbiomass^{-1}), suggesting that the change of reaction temperature and pressurized hydrogen have less effect on the generation of acetic acid. Moreover, the temperature elevated from 200 to 280°C，the selectivity towards EG and 1,2-PG increases, from 5 up to 68 mg•$g_{biomass}^{-1}$ and 16 up to the plateau 58 mg•$g_{biomass}^{-1}$, respectively. It can be explained by the fact that high temperature promotes glucose's C-C bonds to cleave by hydrogenation/hydrogenolysis. 1-hydroxy-2-butanone has similar mass if the temperature above 200°C. It is worthwhile to notice that both tetrahydrofurfuryl alcohol, DMF and ethanol appearance at high H_2 pressure and temperature (30 bar and 250/280°C) or in low H_2 pressure cases (0 and 10 bar), as shown in HPLC curves (Fig.6D and Fig.S6), the reasons for these results are not clear.

3.4.3 Effect of contact time

Increase contact time may enable high conversion or/and yield but can reduce selectivity because of multi-step reactions. Long contact time have indeed been reported for lignin valorization but not in the view of co-depolymerizing cellulose. The effect of contact time on depolymerization was therefore studied under the optimal reaction conditions (20 mL n-butanol, 20 mL water, 2.0 g extracted eucalyptus powder sawdust, 0.2 g Ru/C, 0.4g MgO, 250°C, 30 bar H_2.).

As Fig.8A shown, increasing the contact time (from 2h to 24h) exhibited a little effect on lignin oil yield but did change the yield of total monomers and the selectivity of monomers. The yield of total aromatic monomer increased from 38.89% for 1h, reaching to the top of 68.54% for 6h, and then decreases to 51.21% with prolonged contact time. This change can be explained that lignin and oligomers were degraded and further converted to monomers in the contact time rage of 1~6 h, and the decreasing yield of monomers were ascribed to repolymerization when the contact time longer than 8h. The similar trend was also evidenced in previous reports [74]. Longer time did not enhance lignin oil yield. GPC analysis shows that little high M_W oligomer was detected at the start of the reaction, whereas longer contact time led to high M_W fragments (Fig.S10). Not insignificant, condensation in both hydrogenolysis and alkalin depolymerization cannot be excluded (vide infra) because condensation of unsaturated double bond and carbocation on benzene ring (or Cα in side-chain) has been reported at a long contact time [23]. With reaction time increasing, more coniferyl/sinapyl alcohols released from lignin matrix were converted to G3/S3-OH (pathway P2), G3/S3(pathway P3+P6) and G0/S0 (pathway P3+P8+P9) (Scheme 1). However, Prolonging the contact time, the yield of G3/S3-OH was changed from 22.12% to the highest 35.84% at 6h and then decreased, while was not obvious effect on the selectivity of G3/S3 and G0/S0 monomers (Fig.8A), attributing to the repolymerization of G1/S1=O and coniferyl/sinapyl alcohols [75]. These were also confirmed by GPC analysis (newly produced high M_W fragments, Fig.S10). Moreover, no obvious change of G3/S3 yield also indicates that the formation of G3/S3 (propyl-substituted monomers) occurs

primarily through pathway P3+P6. Whereas the yield of G1/S1 increased with contact time increasing, which is responsible for the decarbonylation of G2/S2=O over alkali-catalyzed [54].

The reaction time also affected the mass of aqueous phase products. The aqueous phase product mass was about 33.30 wt % (based on eucalyptus mass) when the contact time was 1h, and then increased to the highest mass of 63.35 wt % with the contact time increasing to 8 h, but the contact time further increased (8h) gave rise to the aqueous phase product mass decreased. Meanwhile, the mass of oligomers firstly increased and subsequent decreased to complete dissolve and then increased to a plateau (0.05 wt %). The mentioned above variation trends are likely correlated with the magnesium species during depolymerization process, that is, MgO was converted successively to $Mg(OH)_2$, $Mg_5(CO_2)_3(OH)_2{\cdot}4H_2O$ and $MgCO_3$ with the increasing contact time (Fig.S10). These changing magnesium species were also reported and exhibited similar effect on cellulose depolymerization products [21, 52]. They pointed out that Mg (OH) $_2$ derived from MgO thermal conversion improves the ability of cellulose degradation. The aqueous phase monomers were strongly influenced by reaction time. The main aqueous phase products are soluble oligomers, tetrahydrofurfuryl alcohol, ethanol, 1-hydroxy-2-butanone, 1, 2-PG, EG, glycerin and LA (Fig.8B and Fig.S9). Expect for methanol and acetol, the mass of main monomers increased when the contact time increased from 1h to 8h. As the contact time continues to prolong, the mass of total aqueous phase products and most monomers decrease but oligomers appeared again, which are attribute to the change of magnesium species. Meanwhile, some monomers were converted to gas products evidencing was also confirmed by the gas products (Table S2).

3.5 The stability of the solvent and catalyst recycle

To investigate the effect of depolymerization process on the stability of n-butanol solvent, the gaseous and aqueous products were analyzed after conducting the valorization of eucalyptus or without feedstock under 250℃in n-butanol/H_2O for 6h. From the result of GC and GC-MS, a portion of n-butanol was converted whether the feedstock is added or not (Fig. 9, Table S2). Without feedstock, the main components in gaseous phase are H_2, CH_4, C_2H_6 and C_3H_8, suggesting that the activity of catalyst is contributed to cleave C_α–C_β bond in n-butanol for generation a large amount of CH_4 (25.85%) and C_3H_8 (15.18%, not include propane in n-butanol phase (Fig.9)) (Table S2) [39, 76]. A similar reaction of propanol was converted to methane and ethane over hydrogenation catalyst [77]. Butyl butyrate and propane were detected in n-butanol phase (Fig.9), ascribing to esterification taking place between n-butanol and butyric acid (originate from butaldehyde oxidation) over MgO catalyst. Therefore, a portion of n-butanol solvent is converted to propane, methane and butyl butyrate in n-butanol/H_2O solvents over Ru/C-MgO catalysts. However, just a few gaseous products (H_2, CO_2, CO, CH_4, C_3H_8 and C_4H_{10}) were obtained when feedstock was added (Table S2), CO_2, CO came from decarbonylation and decarboxylation reactions. Butyl butyrate and propane were also decrease in n-butanol phase (Fig.9), suggesting that changing the catalyst performance and reducing the catalyst dosage would be reduced the solvent side-reactions [39].

In this work, MgO was converted to $Mg(OH)_2$ during the hydrothermal process and also confirmed by the XRD analysis of the solid mixture (depolymerization residue and catalyst) (Fig. 11). After reaction, we conducted the recycle experiment of catalysts. $Mg(OH)_2$ was located at the bottom of the aqueous phase and calcined at 550℃(6 h) to get MgO for reuse. Meanwhile, the used Ru/C in the n-butanol phase (due to a relatively polar) was isolated and dried at 105℃ (10 h) for reusing with regenerated MgO. In this way, a black powder could be recycled about 97.4 wt% of the initial Ru/C (0.2g), the white powder was afforded about 92.5wt% (viz. 0.37g) of the original MgO (0.4g, Fig. S10). Subsequently, the eucalyptus powder depolymerization experiment (Fig.1) was carried out over the recycled catalysts under the given conditions (fresh catalysts were added to make up for the loss of retrieved catalysts). As Fig.10 shown, the recycled catalysts afforded a decrease lignin oil (24.36 wt% of feedstock) and aromatic monomer yield (56.58 wt% of lignin) compared to fresh Ru/C-MgO (25.50 wt% of feedstock and 68.54wt% of lignin), with a little higher selectivity towards G3/H3-OH monomers (Fig. 10A). Similarly, the obtained aqueous product yield was also slightly lower (596.03 vs. 556.27 mg g^{-1} biomass). The decreasing of lignin oil, monomer yield and aqueous products probably because of the altered property of catalyst, especially MgO. The second run reused catalysts relative characterization was analyzed by XRD. The X-ray diffraction patterns displayed no Ru diffraction peak was detected as fresh catalyst, implying Ru particles were not obviously aggregated. While obvious difference between fresh and used MgO are exhibited as the diffraction peaks shown (PDF # 32-0671, Fig.11). For instance, the evident decrease of MgO diffraction peaks (PDF # 45-0964, periclase) due to the MgO particle become small and a portion of MgO species change the crystal form. To conclude, this recycle experiment confirms that the used Ru/C can be reused with a good catalytic activity and spent MgO was changed with a decline activity.

4. Conclusions

A metal-alkaline catalytic valorization approach is developed, the one-pot complete conversion and separation of woody biomass into two value product streams: lignin derived phenolics and semi-cellulose-derived small molecular (C2~C5) alcohols and acids. Lignocellulose depolymerization is conducted in a mixture of n-butanol/H_2O (homogeneous phase) at 250 °C in metal-alkaline coupling catalytic system. The co-solvent mixture enables extraction and depolymerization of both lignin and hemicellulose, whereas the metal-alkali coupled catalysts enable to cleave inter-/intramolecular linkages of lignocellulose into target products (phenolics, alcohols and acids). Cooling of the reaction liquor gives rise to phase separation, providing an integrated separation of aromatics (n-butanol phase) and small molecular alcohols and acids (aqueous phase). Furthermore, this work exhibits that simultaneous depolymerization all components of lignocellulose in one-pot catalytic refining process is feasible, but one should take into consideration that high product yield and selectivity can hardly without the appropriate reaction conditions. For instance, it was shown that the catalyst, hydrogen pressure, solvent composition, temperature and alkality have different consequences for valorization the main component of biomass.

Declarations

Acknowledgements

This work was supported by Basic scientific research operating expenses project of Key Lab. of Biomass Energy and Material, Jiangsu Province (JSBEM201902), the Natural Science Foundation of Guangdong Province (No.2019A1515012220), the National Key R&D Program of China (2018YFB1501504), the NSFC (Natural Science Foundation of China) project (No.51676191, 51536009).

References

[1] Bastin, J. F.; Finegold, Y.; Garcia, C., et al., The global tree restoration potential [J]. Science **2019,** 365 (6448), 76-79.

[2] Li, C.; Zhao, X.; Wang, A., et al., Catalytic Transformation of Lignin for the Production of Chemicals and Fuels [J]. Chemical reviews **2015,** 115 (21), 11559-11624.

[3] Lin, Y. C.; Huber, G. W., The critical role of heterogeneous catalysis in lignocellulosic biomass conversion [J]. Energ Environ Sci **2009,** 2 (1), 68-80.

[4] Ferrini, P.; Rinaldi, R., Catalytic Biorefining of Plant Biomass to Non-Pyrolytic Lignin Bio-Oil and Carbohydrates through Hydrogen Transfer Reactions [J]. Angew Chem Int Edit **2014,** 53 (33), 8634-8639.

[5] Sun, Z. H.; Fridrich, B.; de Santi, A., et al., Bright Side of Lignin Depolymerization: Toward New Platform Chemicals [J]. Chemical reviews **2018,** 118 (2), 614-678.

[6] Borrero-Lopez, A. M.; Santiago-Medina, F. J.; Valencia, C., et al., Valorization of Kraft Lignin as Thickener in Castor Oil for Lubricant Applications [J]. J Renew Mater **2018,** 6 (4), 347-361.

[7] Liao, Y. H.; Koelewijn, S. F.; Van den Bossche, G., et al., A sustainable wood biorefinery for low-carbon footprint chemicals production [J]. Science **2020,** 367 (6484), 1385-1390.

[8] Binder, J. B.; Raines, R. T., Simple Chemical Transformation of Lignocellulosic Biomass into Furans for Fuels and Chemicals [J]. J Am Chem Soc **2009,** 131 (5), 1979-1985.

[9] Shen, D. K.; Jin, W.; Hu, J., et al., An overview on fast pyrolysis of the main constituents in lignocellulosic biomass to valued-added chemicals: Structures, pathways and interactions [J]. Renew Sust Energ Rev **2015,** 51, 761-774.

[10] Zhang, Y. Q.; He, H. Y.; Liu, Y. R., et al., Recent progress in theoretical and computational studies on the utilization of lignocellulosic materials [J]. Green Chem **2019,** 21 (1), 9-35.

[11] Liu, Y.; Nie, Y.; Lu, X., et al., Cascade utilization of lignocellulosic biomass to high-value products [J]. Green Chem **2019,** 21 (13), 3499-3535.

[12] Sun, Z. H.; Bottari, G.; Afanasenko, A., et al., Complete lignocellulose conversion with integrated catalyst recycling yielding valuable aromatics and fuels [J]. Nat Catal **2018,** 1 (1), 82-92.

[13] Liu, X. H.; Wang, C. G.; Zhang, Y., et al., Selective Preparation of 4-Alkylphenol from Lignin-Derived Phenols and Raw Biomass over Magnetic Co-Fe@N-Doped Carbon Catalysts [J]. Chemsuschem **2019,** 12 (21), 4791-4798.

[14] Kuna, E.; Behling, R.; Valange, S., et al., Sonocatalysis: A Potential Sustainable Pathway for the Valorization of Lignocellulosic Biomass and Derivatives [J].Topics Curr Chem **2017,** 375 (2). DOI:10.1007/s41061-017-0122-y.

[15] Wang, H. Y.; Zhu, C. H.; Li, D., et al., Recent advances in catalytic conversion of biomass to 5-hydroxymethylfurfural and 2, 5-dimethylfuran [J]. Renew Sust Energ Rev **2019,** 103, 227-247.

[16] Liu, Q. Y.; Wang, H. Y.; Xin, H. S., et al., Selective Cellulose Hydrogenolysis to Ethanol Using Ni@C Combined with Phosphoric Acid Catalysts [J]. Chemsuschem **2019,** 12 (17), 3977-3987.

[17] Wang, H. Y.; Zhu, C. H.; Liu, Q. Y., et al., Selective Conversion of Cellulose to Hydroxyacetone and 1-Hydroxy-2-Butanone with Sn-Ni Bimetallic Catalysts [J]. Chemsuschem **2019,** 12 (10), 2154-2160.

[18] Song, H. Y.; Wang, P.; Li, S., et al., Direct conversion of cellulose into ethanol catalysed by a combination of tungstic acid and zirconia-supported Pt nanoparticles [J]. Chem Commun **2019,** 55 (30), 4303-4306.

[19] Huber, G. W.; Iborra, S.; Corma, A., Synthesis of transportation fuels from biomass: Chemistry, catalysts, and engineering [J]. Chemical reviews **2006,** 106 (9), 4044-4098.

[20] Ji, N.; Zhang, T.; Zheng, M. Y., et al., Direct Catalytic Conversion of Cellulose into Ethylene Glycol Using Nickel-Promoted Tungsten Carbide Catalysts [J]. Angew Chem Int Edit **2008,** 47 (44), 8510-8513.

[21] Zhang, Y. H.; Wang, A. Q.; Zhang, T., A new 3D mesoporous carbon replicated from commercial silica as a catalyst support for direct conversion of cellulose into ethylene glycol [J]. Chem Commun **2010,** 46 (6), 862-864.

[22] Li, C.; Xu, G. Y.; Li, K., et al., A weakly basic Co/CeOx catalytic system for one-pot conversion of cellulose to diols: Kungfu on eggs [J]. Chem Commun **2019,** 55 (53), 7663-7666.

[23] Yuting Zhu, Y. L., Wei Lv, Jing Liu, Xiangbo Song, Lungang Chen, Chenguang Wang,*; Bert F. Sels, a. L. M., Complementing Vanillin and Cellulose Production by Oxidation of Lignocellulose with Stirring Control [J]. ACS Sustainable Chem. Eng. **2020,** (8), 2361−2374.

[24] Wang, C. Y.; Sun, J.; Tao, Y. Q., et al., Biomass materials derived from anethole: conversion and application [J]. Polym Chem-Uk **2020,** 11 (5), 954-963.

[25] Zakzeski, J.; Bruijnincx, P. C. A.; Jongerius, A. L., et al., The Catalytic Valorization of Lignin for the Production of Renewable Chemicals [J]. Chemical reviews **2010,** 110 (6), 3552-3599.

[26] Schutyser, W.; Renders, T.; Van den Bosch, S., et al., Chemicals from lignin: an interplay of lignocellulose fractionation, depolymerisation, and upgrading [J]. Chemical Society reviews **2018,** 47 (3), 852-908.

[27] Gandini, A., The irruption of polymers from renewable resources on the scene of macromolecular science and technology [J]. Green Chem **2011,** 13 (5), 1061-1083.

[28] Ragauskas, A. J.; Beckham, G. T.; Biddy, M. J., et al., Lignin Valorization: Improving Lignin Processing in the Biorefinery [J]. Science **2014,** 344 (6185), 709-710.

[29] Zhao, C.; Kou, Y.; Lemonidou, A. A., et al., Highly Selective Catalytic Conversion of Phenolic Bio-Oil to Alkanes [J]. Angew Chem Int Edit **2009,** 48 (22), 3987-3990.

[30] Ha, Y. B.; Jin, M. Y.; Oh, S. S., et al., Synthesis of an Environmentally Friendly Phenol-Free Resin for Printing Ink [J]. B Korean Chem Soc **2012,** 33 (10), 3413-3416.

[31] Yuhe Liao*, S.-F. K., Gil Van den Bossche, Joost Van Aelst, Sander Van den Bosch, Tom Renders, Kranti Navare, Thomas Nicolaï, Korneel Van Aelst1, Maarten Maesen4, Hironori Matsushima, Johan Thevelein3, Karel Van Acker, Bert Lagrain, Danny Verboekend, Bert F. Sels*, A sustainable wood biorefinery for low–carbon footprint chemicals production [J]. Science **2020,** 367 (6484), 1385-1390.

[32] Van den Bosch, S.; Schutyser, W.; Koelewijn, S. F., et al., Tuning the lignin oil OH-content with Ru and Pd catalysts during lignin hydrogenolysis on birch wood [J]. Chem Commun (Camb) **2015,** 51 (67), 13158-13161.

[33] Alonso, D. M.; Hakim, S. H.; Zhou, S. F., et al., Increasing the revenue from lignocellulosic biomass: Maximizing feedstock utilization [J]. Science Advances **2017,** 3 (5). DOI: 10.1126/sciadv.1603301.

[34] Li, C. Z.; Zheng, M. Y.; Wang, A. Q., et al., One-pot catalytic hydrocracking of raw woody biomass into chemicals over supported carbide catalysts: simultaneous conversion of cellulose, hemicellulose and lignin [J]. Energ Environ Sci **2012,** 5 (4), 6383-6390.

[35] Li, X. C.; Guo, T. Y.; Xia, Q. N., et al., One-Pot Catalytic Transformation of Lignocellulosic Biomass into Alkylcyclohexanes and Polyols [J]. Acs Sustain Chem Eng **2018,** 6 (3), 4390-4399.

[36] Liu, Y.; Chen, L. G.; Wang, T. J., et al., One-Pot Catalytic Conversion of Raw Lignocellulosic Biomass into Gasoline Alkanes and Chemicals over LiTaMoO6 and Ru/C in Aqueous Phosphoric Acid [J]. Acs Sustain Chem Eng **2015,** 3 (8), 1745-1755.

[37] A. Sluiter, B. H., R. Ruiz, C. Scarlata, J. Sluiter, D. Templeton, Crocker D, Determination of structural carbohydrates and lignin in biomass [J]. http://wwwnrelgov/biomass/analytical_procedureshtml**2008**.

[38] Renders, T.; Schutyser, W.; Van den Bosch, S., et al., Influence of Acidic (H3PO4) and Alkaline (NaOH) Additives on the Catalytic Reductive Fractionation of Lignocellulose [J]. Acs Catal **2016,** 6 (3), 2055-2066.

[39] Renders, T.; Cooreman, E.; Van den Bosch, S., et al., Catalytic lignocellulose biorefining in n-butanol/water: a one-pot approach toward phenolics, polyols, and cellulose [J]. Green Chem., 2018, 20, 4607–4619. DOI: 10.1039/C8GC01031E.

[40] Verboekend, D.; Liao, Y.; Schutyser, W., et al., Alkylphenols to phenol and olefins by zeolite catalysis: a pathway to valorize raw and fossilized lignocellulose [J]. Green Chem. **2016,** 18 (1), 297-306.

[41] He, J. Y.; Zhao, C.; Lercher, J. A., Impact of solvent for individual steps of phenol hydrodeoxygenation with Pd/C and HZSM-5 as catalysts [J]. J Catal **2014,** 309, 362-375.

[42] He, J. Y.; Zhao, C.; Mei, D. H., et al., Mechanisms of selective cleavage of C-O bonds in di-aryl ethers in aqueous phase [J]. J Catal **2014,** 309, 280-290.

[43] Ma, W. L. Y. L. Y. Z. J. L. C. Z. C. W. Y. X. Q. Z. G. C. L., The effect of Ru/C and MgCl2 on the cleavage of interand intra-molecular linkages during cornstalk hydrolysis residue valorization [J]. Cellulose **2020,** 27 (2), 799-823.

[44] Lv, W.; Si, Z.; Tian, Z. P., et al., Synergistic Effect of EtOAc/H2O Biphasic Solvent and Ru/C Catalyst for Cornstalk Hydrolysis Residue Depolymerization [J]. Acs Sustain Chem Eng **2017,** 5 (4), 2981-2993.

[45] Chen, J. Z.; Lu, F.; Si, X. Q., et al., High Yield Production of Natural Phenolic Alcohols from Woody Biomass Using a Nickel-Based Catalyst [J]. Chemsuschem **2016,** 9 (23), 3353-3360.

[46] Renders, T.; Van den Bosch, S.; Vangeel, T., et al., Synergetic Effects of Alcohol/Water Mixing on the Catalytic Reductive Fractionation of Poplar Wood [J]. Acs Sustain Chem Eng **2016,** 4 (12), 6894-6904.

[47] Maczynski, A.; Shaw, D. G.; Goral, M., et al., IUPAC-NIST solubility data series. 82. Alcohols with water-revised and updated: Part 1. C-4 alcohols with water [J]. J Phys Chem Ref Data **2007,** 36 (1), 59-132.

[48] Barton, A. F., Alcohols with Water: Solubility Data Series [J]. Elsevier **2013**.

[49] Anderson, E. M.; Stone, M. L.; Katahira, R., et al., Flowthrough Reductive Catalytic Fractionation of Biomass [J]. Joule **2017,** 1 (3), 613-622.

[50] Kumaniaev, I.; Subbotina, E.; Savmarker, J., et al., Lignin depolymerization to monophenolic compounds in a flow-through system [J]. Green Chem **2017,** 19 (24), 5767-5771.

[51] Anderson, E. M.; Stone, M. L.; Hulsey, M. J., et al., Kinetic Studies of Lignin Solvolysis and Reduction by Reductive Catalytic Fractionation Decoupled in Flow-Through Reactors [J]. Acs Sustain Chem Eng **2018,** 6 (6), 7951-7959.

[52] Nakagawa, Y.; Ishikawa, M.; Tamura, M., et al., Selective production of cyclohexanol and methanol from guaiacol over Ru catalyst combined with MgO [J]. Green Chem **2014,** 16 (4), 2197-2203.

[53] Aiqin Wang; Tao, Z., One-Pot Conversion of Cellulose to Ethylene Glycol with Multifunctional Tungsten- Based Catalysts [J]. Acc. Chem. Res. 2013, 46, 7, 1377–1386.

[54] Wei Lv, Y. Z., Longlong Ma, et al., Modifying MgO with Carbon for Valorization of Lignin to Aromatics [J]. ACS Sustainable Chem. Eng. **2019,** 7, 5751−5763.

[55] Yan, X. Y.; Jin, F. M.; Tohji, K., et al., Hydrothermal Conversion of Carbohydrate Biomass to Lactic Acid [J]. Aiche J **2010,** 56 (10), 2727-2733.

[56] Jin, F. M.; Yun, J.; Li, G. M., et al., Hydrothermal conversion of carbohydrate biomass into formic acid at mild temperatures [J]. Green Chem **2008,** 10 (6), 612-615.

[57] Jin, F. M.; Enomoto, H., Rapid and highly selective conversion of biomass into value-added products in hydrothermal conditions: chemistry of acid/base-catalysed and oxidation reactions [J]. Energ Environ Sci **2011,** 4 (2), 382-397.

[58] Zhang, J.; Liu, X.; Sun, M., et al., Direct Conversion of Cellulose to Glycolic Acid with a Phosphomolybdic Acid Catalyst in a Water Medium [J]. Acs Catal **2012,** 2 (8), 1698-1702.

[59] Debruijn, J. M.; Kieboom, A. P. G.; Vanbekkum, H., Alkaline-Degradation of Monosaccharides .5. Kinetics of the Alkaline Isomerization and Degradation of Monosaccharides [J]. Recl Trav Chim Pay B **1987,** 106 (2), 35-43.

[60] Yang, B. Y.; Montgomery, R., Alkaline degradation of glucose: Effect of initial concentration of reactants [J]. Carbohyd Res **1996,** 280 (1), 27-45.

[61] Ding, K. F.; Le, Y.; Yao, G. D., et al., A rapid and efficient hydrothermal conversion of coconut husk into formic acid and acetic acid [J]. Process Biochem **2018,** 68, 131-135.

[62] Palkovits, R.; Tajvidi, K.; Ruppert, A. M., et al., Heteropoly acids as efficient acid catalysts in the one-step conversion of cellulose to sugar alcohols [J]. Chem Commun **2011,** 47 (1), 576-578.

[63] Deng, W. P.; Tan, X. S.; Fang, W. H., et al., Conversion of Cellulose into Sorbitol over Carbon Nanotube-Supported Ruthenium Catalyst [J]. Catal Lett **2009,** 133 (1-2), 167-174.

[64] Dietrich, K.; Hernandez-Mejia, C.; Verschuren, P., et al., One-Pot Selective Conversion of Hemicellulose to Xylitol [J]. Org Process Res Dev **2017,** 21 (2), 165-170.

[65] Ennaert, T.; Feys, S.; Hendrikx, D., et al., Reductive splitting of hemicellulose with stable ruthenium-loaded USY zeolites [J]. Green Chem **2016,** 18 (19), 5295-5304.

[66] Geboers, J. A.; Van de Vyver, S.; Ooms, R., et al., Chemocatalytic conversion of cellulose: opportunities, advances and pitfalls [J]. Catal Sci Technol **2011,** 1 (5), 714-726.

[67] Murzin, D. Y.; Kusema, B.; Murzina, E. V., et al., Hemicellulose arabinogalactan hydrolytic hydrogenation over Ru-modified H-USY zeolites [J]. J Catal **2015,** 330, 93-105.

[68] Manaenkov, O. V.; Mann, J. J.; Kislitza, O. V., et al., Ru-Containing Magnetically Recoverable Catalysts: A Sustainable Pathway from Cellulose to Ethylene and Propylene Glycols [J]. Acs Appl Mater Inter **2016,** 8 (33), 21285-21293.

[69] Liao, Y. H.; Liu, Q. Y.; Wang, T. J., et al., Zirconium phosphate combined with Ru/C as a highly efficient catalyst for the direct transformation of cellulose to C-6 alditols [J]. Green Chem **2014,** 16 (6), 3305-3312.

[70] Deng, J.; Ren, P. J.; Deng, D. H., et al., Highly active and durable non-precious-metal catalysts encapsulated in carbon nanotubes for hydrogen evolution reaction [J]. Energ Environ Sci **2014,** 7 (6), 1919-1923.

[71] Liu, W. G.; Chen, Y. J.; Qi, H. F., et al., A Durable Nickel Single-Atom Catalyst for Hydrogenation Reactions and Cellulose Valorization under Harsh Conditions [J]. Angew Chem Int Edit **2018,** 57 (24), 7071-7075.

[72] Deng, T. Y.; Liu, H. C., Direct conversion of cellulose into acetol on bimetallic Ni-SnOx/Al2O3 catalysts [J]. J Mol Catal a-Chem **2014,** 388, 66-73.

[73] Bernas, H.; Plomp, A. J.; Bitter, J. H., et al., Influence of reaction parameters on the hydrogenolysis of hydroxymatairesinol over carbon nanofibre supported palladium catalysts [J]. Catal Lett **2008,** 125 (1-2), 8-13.

[74] Huang, X. M.; Gonzalez, O. M. M.; Zhu, J. D., et al., Reductive fractionation of woody biomass into lignin monomers and cellulose by tandem metal triflate and Pd/C catalysis [J]. Green Chem **2017,** 19 (1), 175-187.

[75] Deuss, P. J.; Scott, M.; Tran, F., et al., Aromatic Monomers by in Situ Conversion of Reactive Intermediates in the Acid-Catalyzed Depolymerization of Lignin [J]. J Am Chem Soc **2015,** 137 (23), 7456-7467.

[76] Van den Bosch, S.; Schutyser, W.; Vanholme, R., et al., Reductive lignocellulose fractionation into soluble lignin-derived phenolic monomers and dimers and processable carbohydrate pulps [J]. Energy Environ. Sci. **2015,** 8 (6), 1748-1763.

[77] Lan, W.; Amiri, M. T.; Hunston, C. M., et al., Protection Group Effects During alpha,gamma-Diol Lignin Stabilization Promote High-Selectivity Monomer Production [J]. Angew Chem Int Edit **2018,** 57 (5), 1356-1360.

Figures

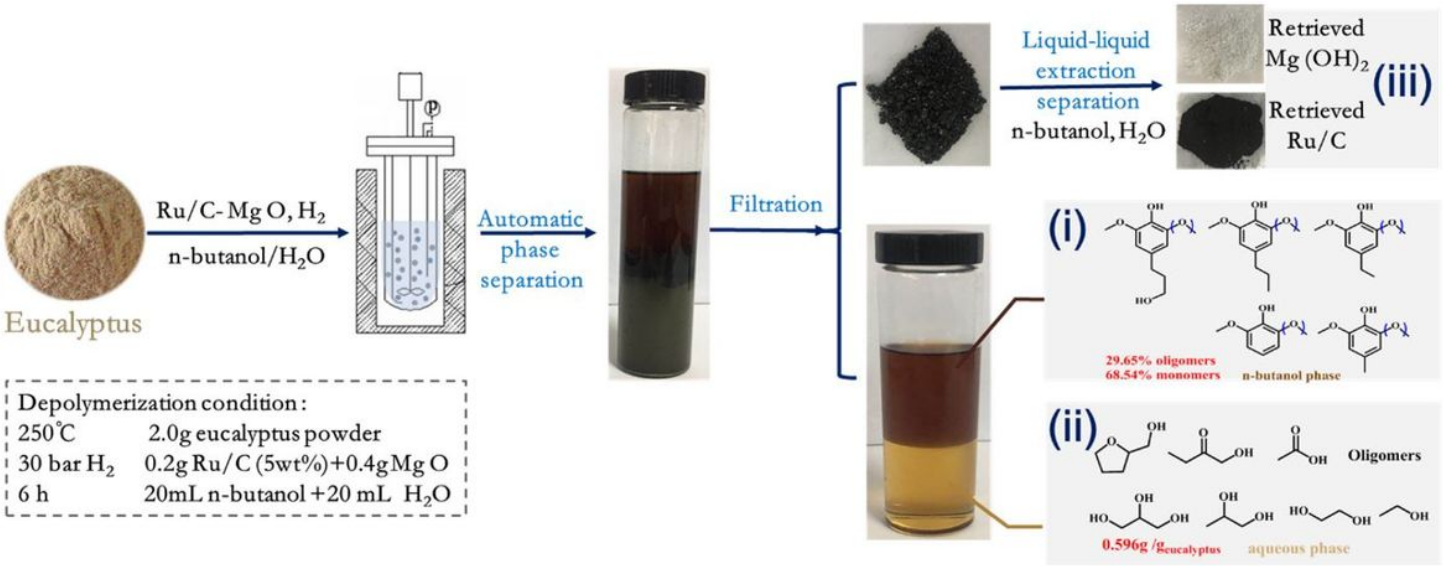

Figure 1

The scheme of depolymerization eucalyptus powder over Ru/C-MgO in a mixture of n-butanol/H2O solvents process targeting (i) lignin-derived aromatics, (ii) small molecular (C2~C5) acids and alcohols, (iii) retrieved Ru/C and Mg(OH)2.

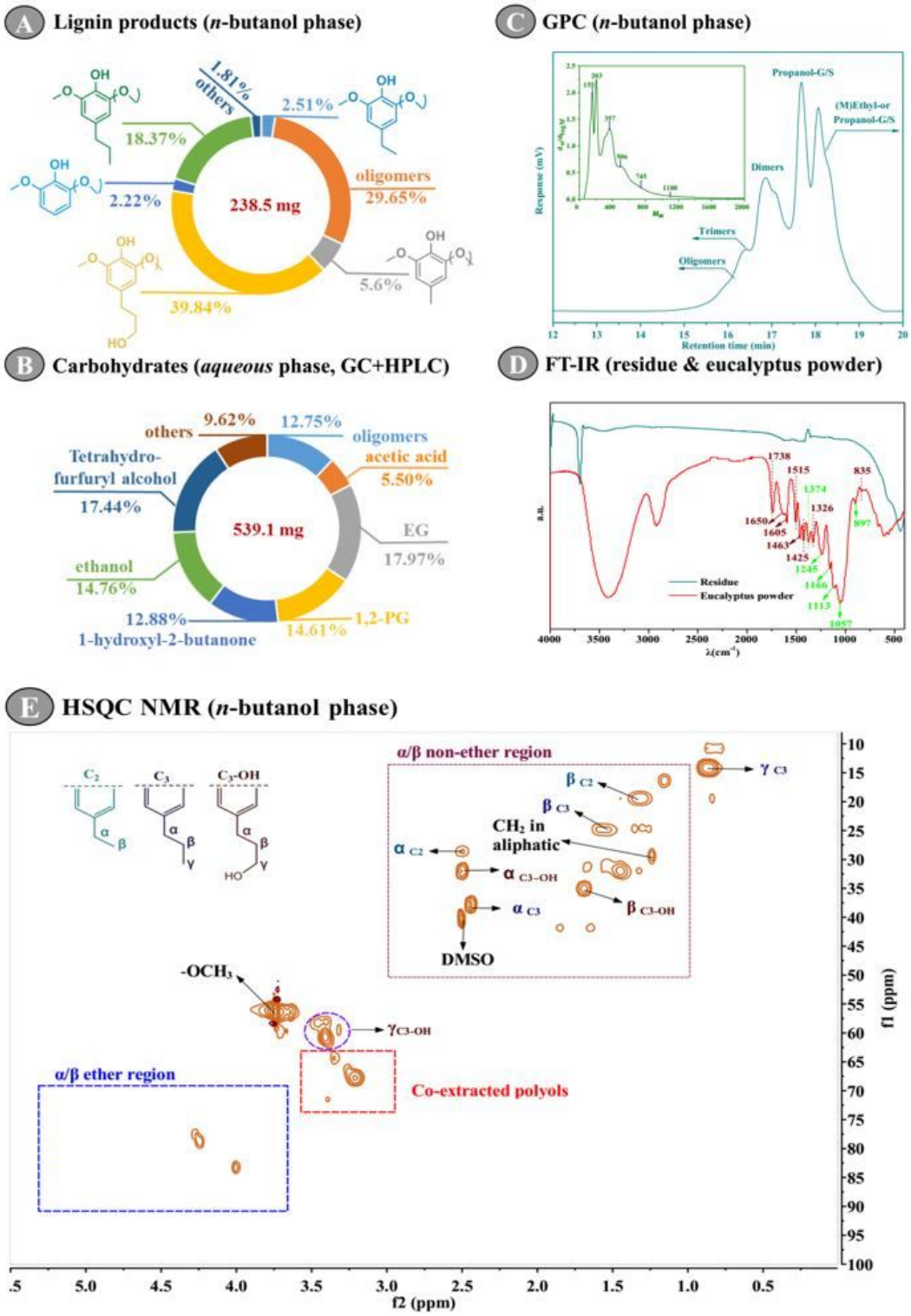

Figure 2

Analysis of the n-butanol phase, aqueous phase and residue obtained from eucalyptus valorization over Ru/C combined with MgO catalysts. Reaction conditions: 20 mL n-butanol, 20 mL water, 2.0 g extracted eucalyptus powder, 0.2 g Ru/C and 0.4g MgO catalysts, 30 bar H2, 250 °C, 6 h. The yield of products were calculated according to the calculation formulas in supporting information. The n-butanol phase products are qualitatively and quantitatively analyzed by GC-MS and GC spectrometers, and the aqueous

phase products are qualitatively and quantitatively analyzed with GC-MS and HPLC spectrometers. (A) Lignin depolymerization product yield, expressed as mg products per g eucalyptus. Acetic acid, EG and 1, 2-PG in n-butanol phase were not included in Fig.2A. (B) Yield of cellulose and hemicellulose depolymerization products in aqueous phase, expressed as mg per g biomass, while the monomer aromatics in aqueous phase were not contained in Fig.2B. See Fig. S9 for HPLC analysis. (C) GPC analysis of non-volatile fractions of n-butanol phase, inset a corresponding Mw-dw/dlogM graph. (D) FT-IR analysis of material and depolymerization residue. (E) HSQC NMR of non-volatile fractions of n-butanol phase.

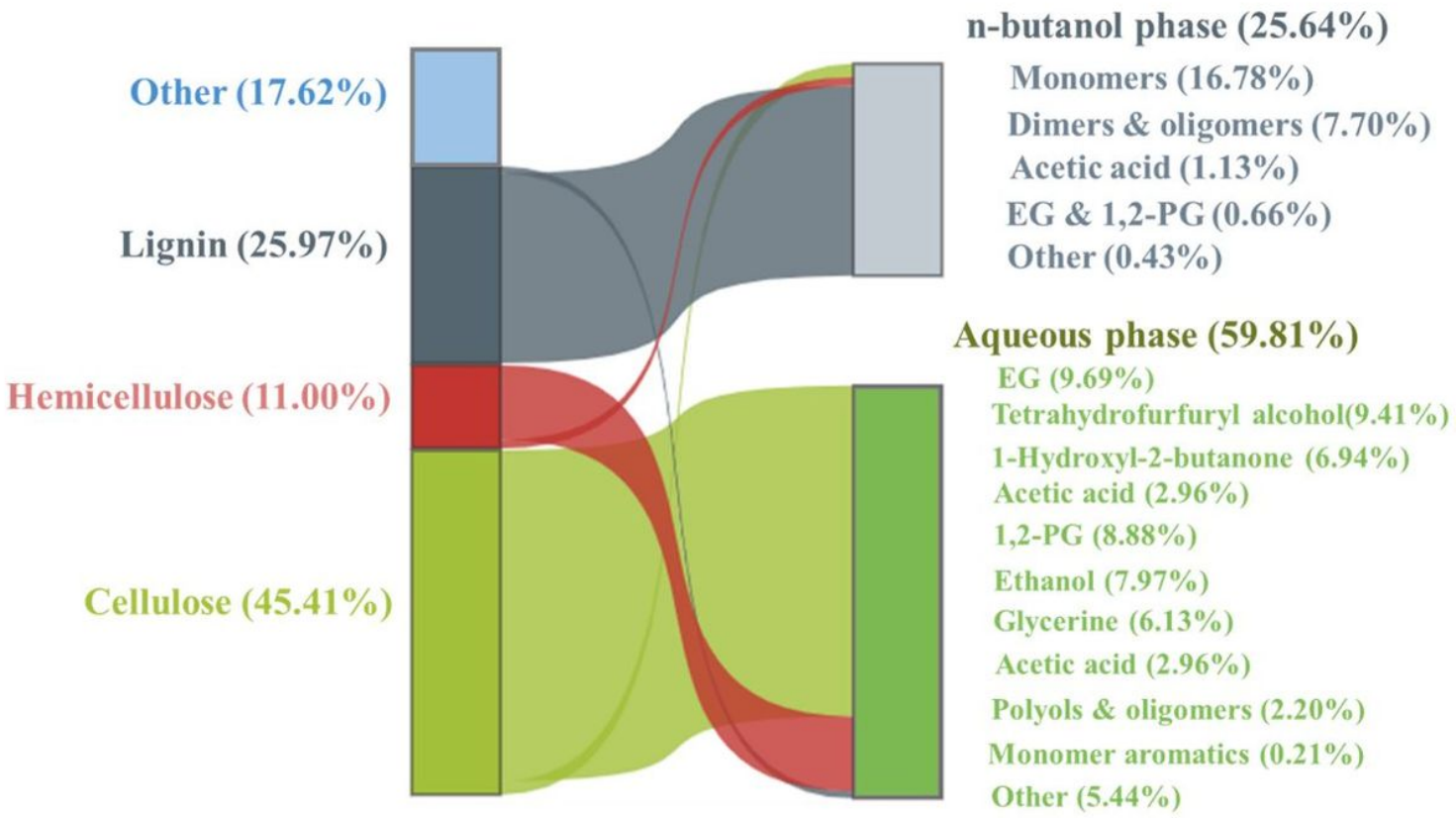

Figure 3

Mass flowchart of the valorization of eucalyptus over Ru/C combined with MgO catalyst

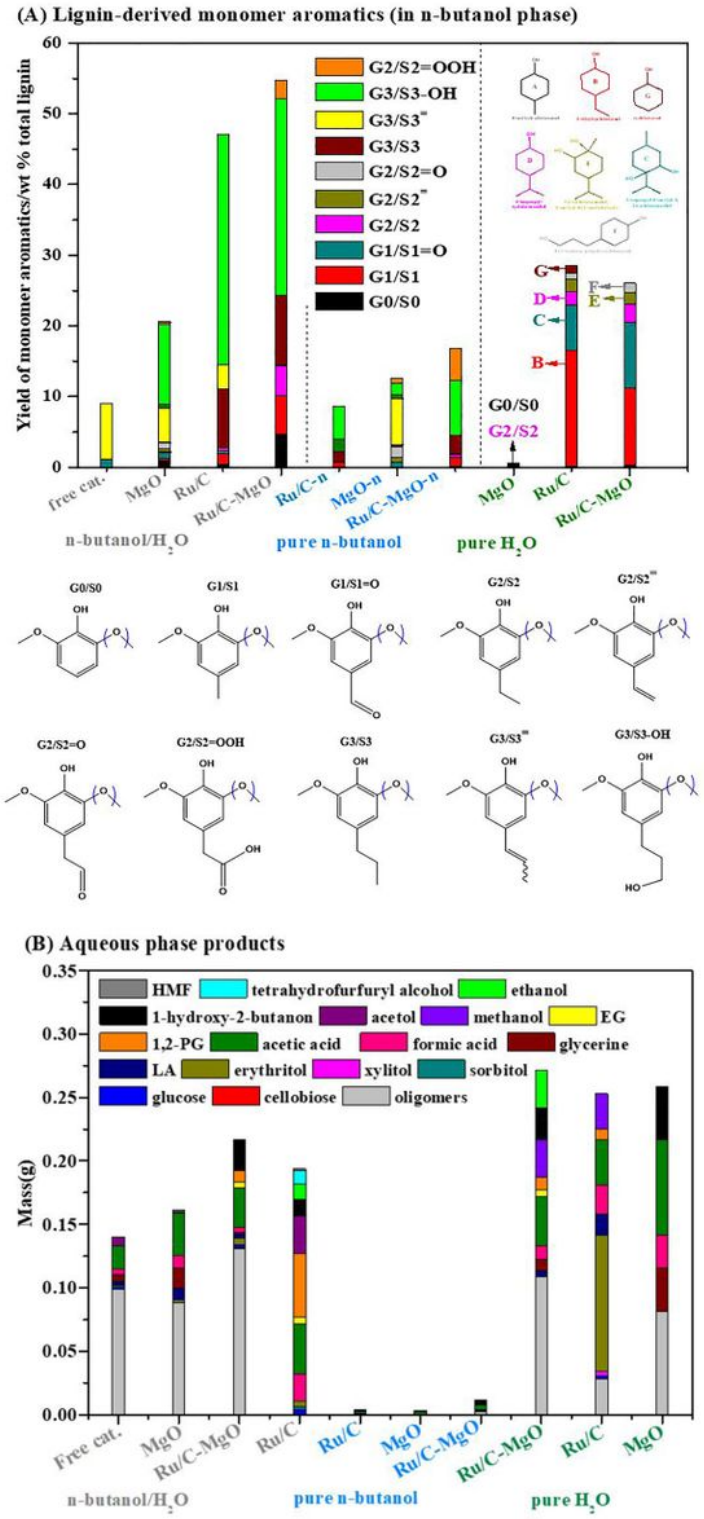

Figure 4

(A) Lignin monomers, (B) carbohydrate products obtained from catalytic depolymerization in n-butanol/water with different catalysts. Reaction conditions: 20 mL n-butanol, 20 mL water, or 40 mL pure n-butanol, or 40 mL pure water, 2.0 g extracted eucalyptus powder sawdust, 0.2 g catalyst, 0.4g MgO, 30 bar H2, 200 °C, 2 h.

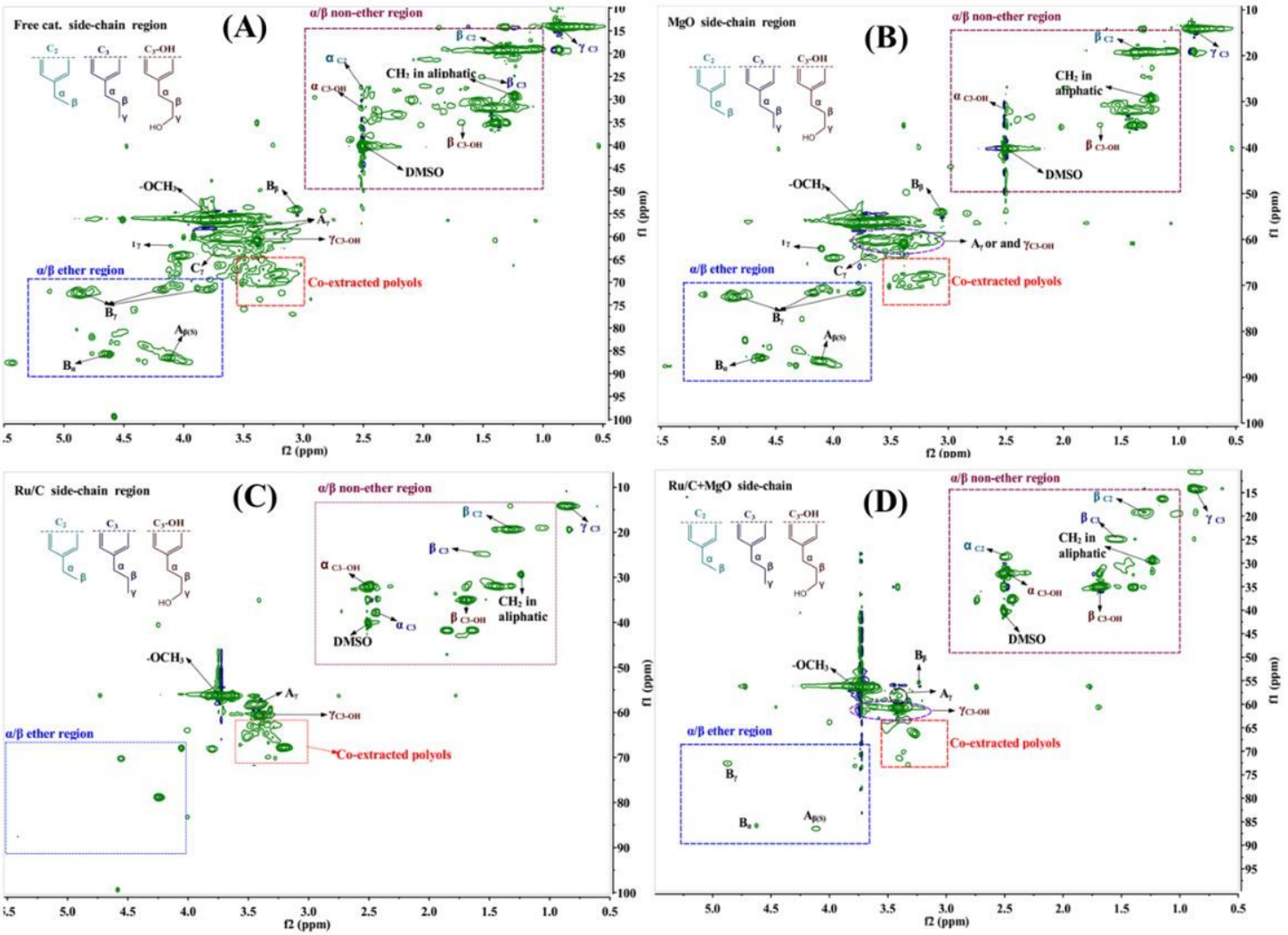

Figure 5

HSQC analysis of the non-volatile lignin oil (n-butanol phase) for different catalysts, (A) Free catalyst, (B) MgO, (C) Ru/C, (D) Ru/C-MgO. Reaction conditions: 2.0 g extracted eucalyptus powder, 0.2 g Ru/C, 0.4g MgO, 20 mL n-butanol, 20 mL water, 30 bar H2, 200 °C, 2 h.

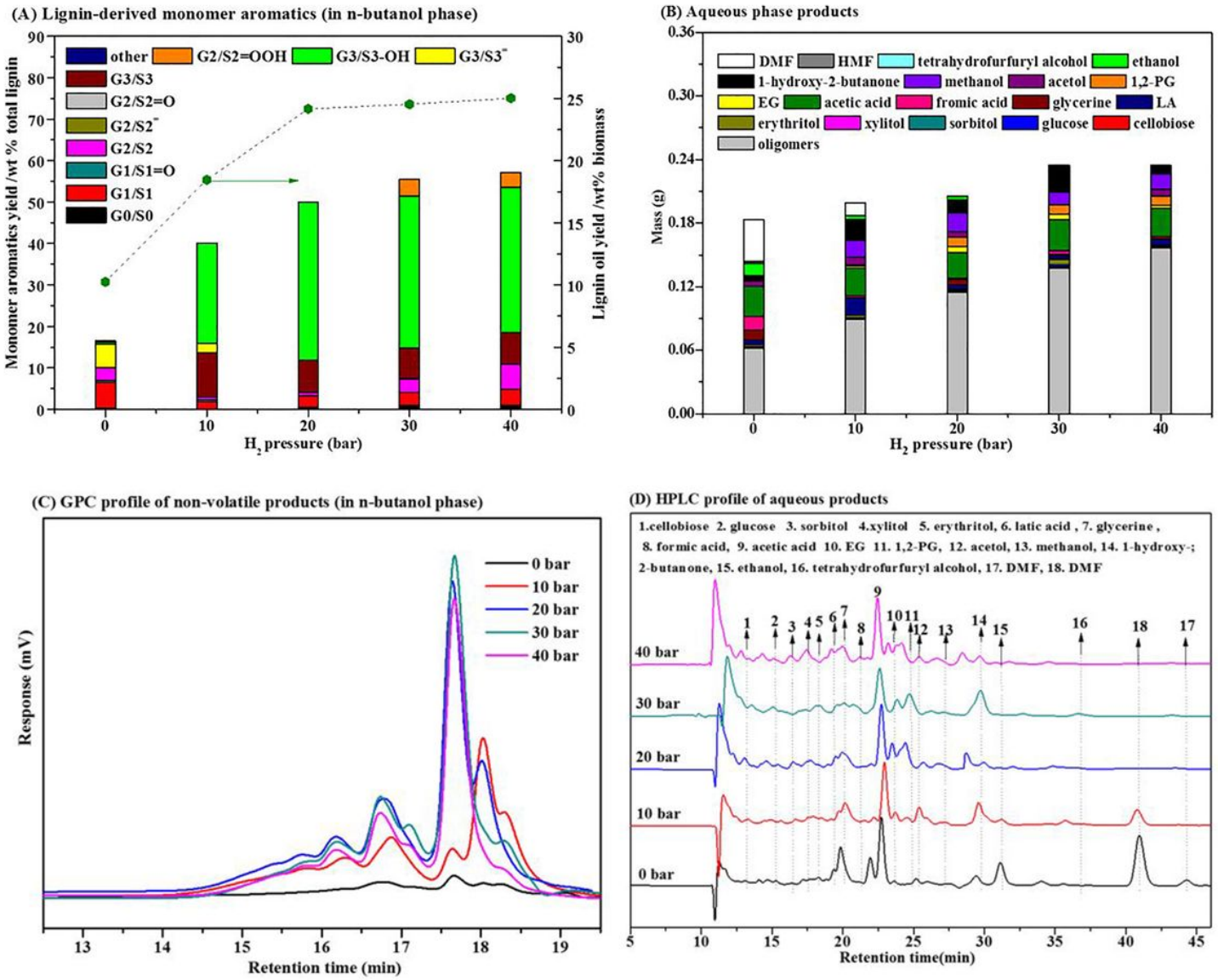

Figure 6

(A) Lignin monomers, (B) carbohydrate products obtained from catalytic depolymerization in n-butanol/water under different H2 pressure, (C) GPC analysis of non-volatile fractions in n-butanol phase, (D) HPLC analysis of fractions in aqueous phase. Reaction conditions: 20 mL n-butanol, 20 mL water, 2.0 g extracted eucalyptus powder sawdust, 0.2 g catalyst, 0.4g MgO, 0~40 bar H2, 200 °C, 2 h.

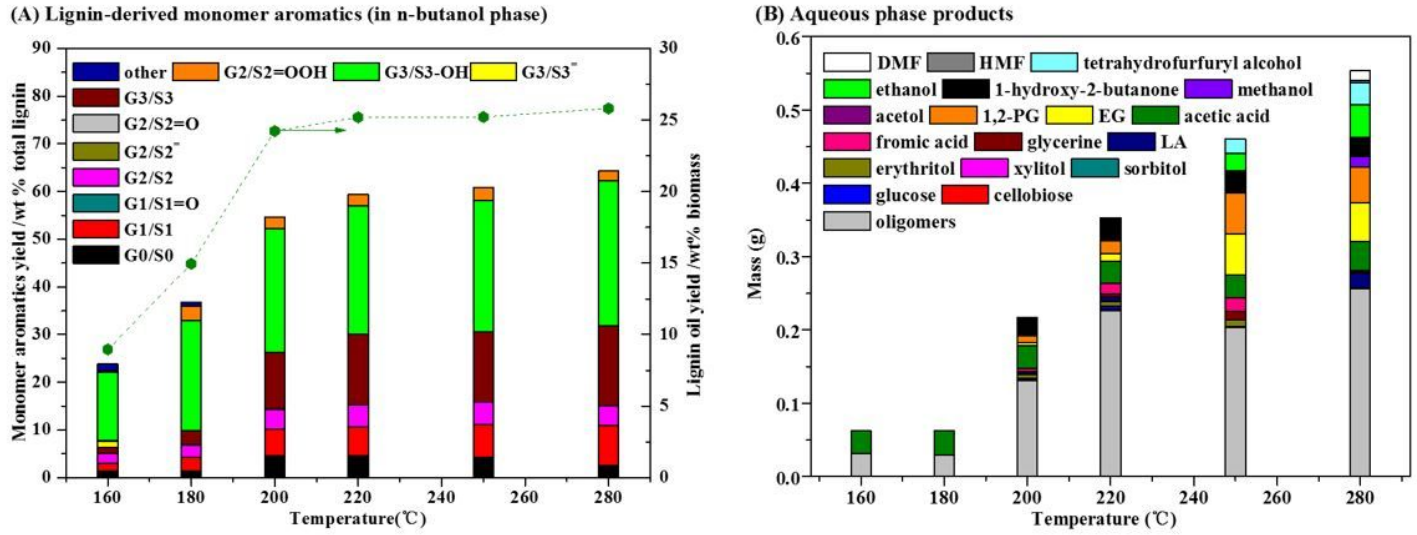

Figure 7

(A) Lignin monomers, (B) carbohydrate products obtained from catalytic depolymerization in n-butanol/water under different temperature. Reaction conditions: 20 mL n-butanol, 20 mL water, 2.0 g extracted eucalyptus powder sawdust, 0.2 g catalyst, 0.4g MgO, 160~280°C, 30 bar H2, 2 h.

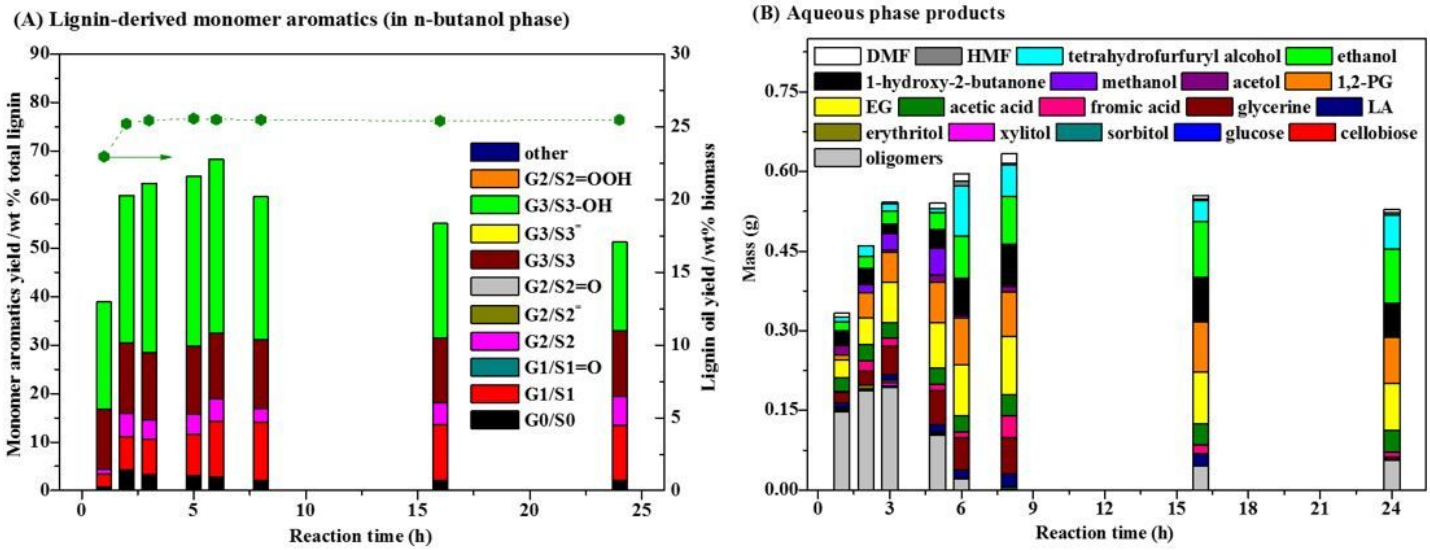

Figure 8

(A) Lignin-derived monomer aromatics, (B) carbohydrate products obtained from catalytic depolymerization in n-butanol/H2O under different contact time. Reaction conditions: 20 mL n-butanol, 20 mL water, 2.0 g non-extracted eucalyptus powder sawdust, 0.2 g catalyst, 0.4g MgO, 250°C, 30 bar H2, 1~24 h.

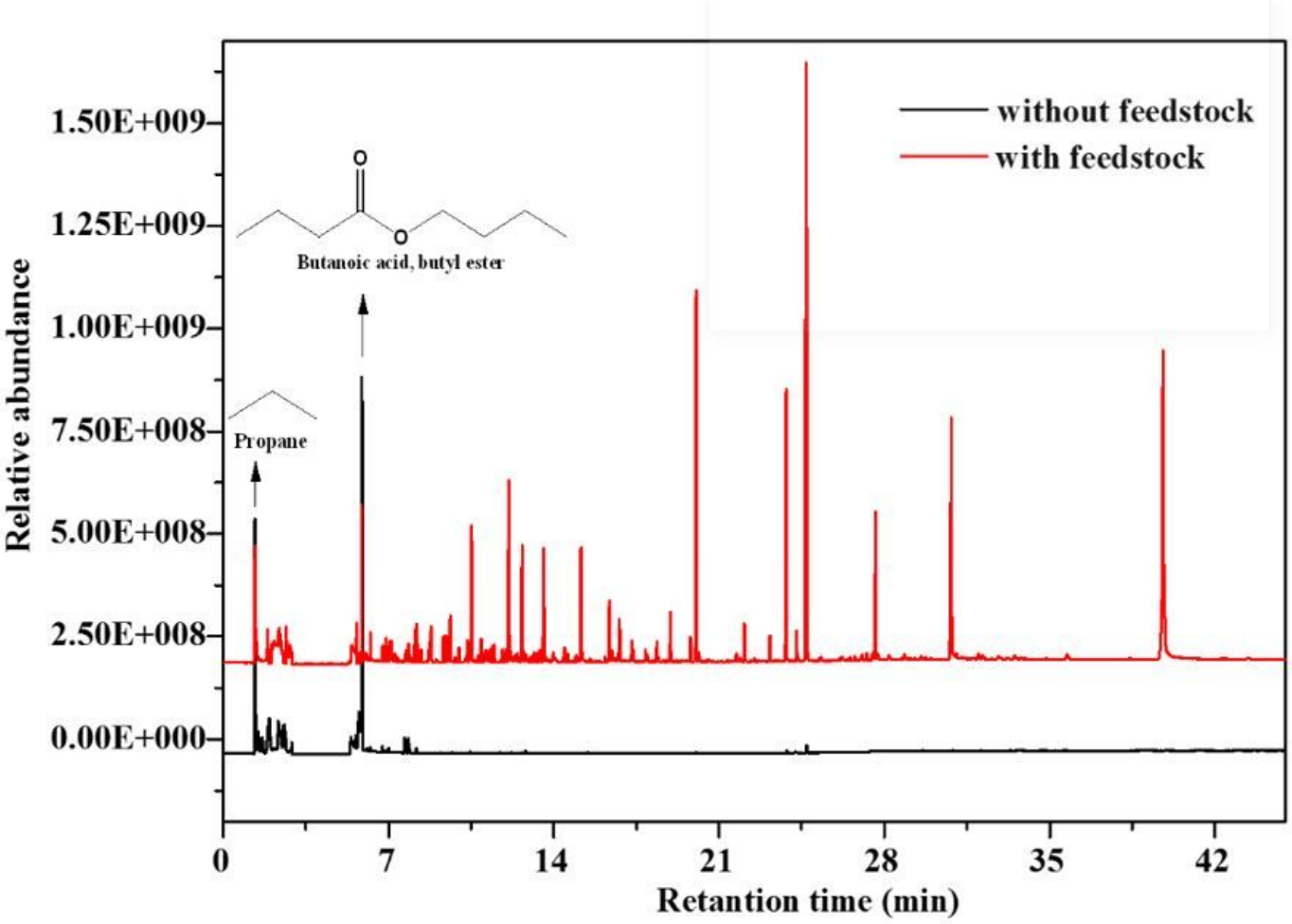

Figure 9

Total-ion chromatogram (TIC) of the n-butanol phase products. Reaction conditions: 20.0 mL n-butanol, 20.0 mL water, (without) eucalyptus powder (1.0 g), 0.2 g Ru/C and 0.4g MgO catalysts, 30 bar H2, 250 °C, 6 h.

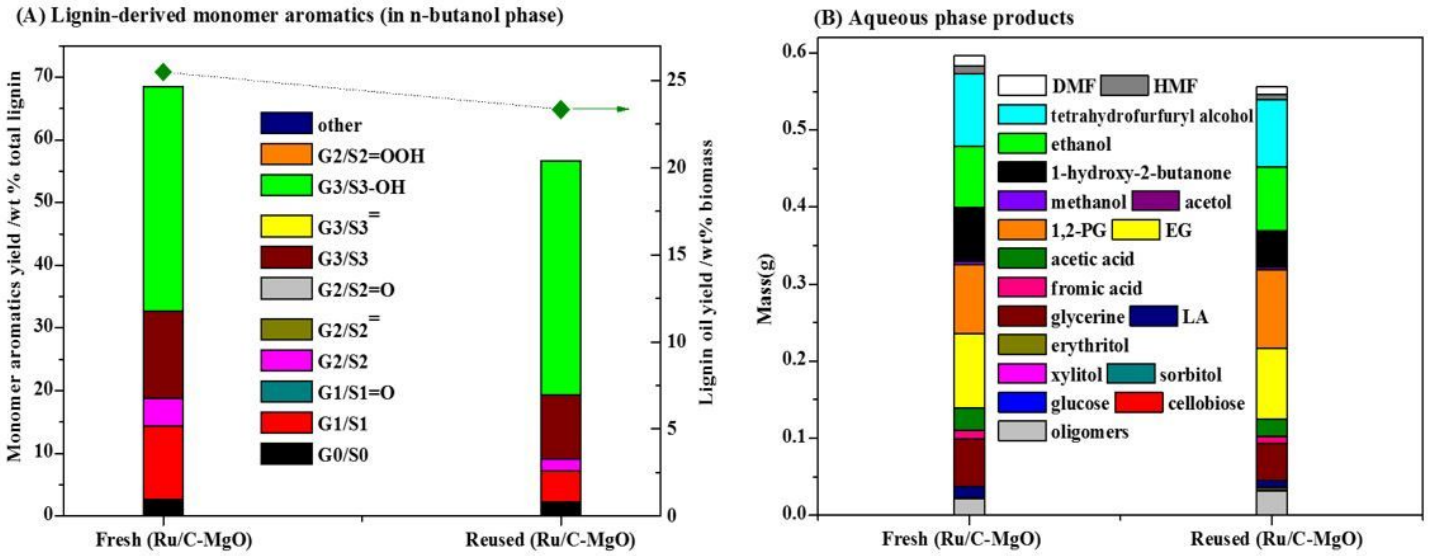

Figure 10

(A) Lignin monomers, (B) carbohydrate products obtained from catalytic depolymerization in n-butanol/water over fresh and reused (Ru/C-MgO) catalysts. Reaction conditions: 20 mL n-butanol, 20 mL water,

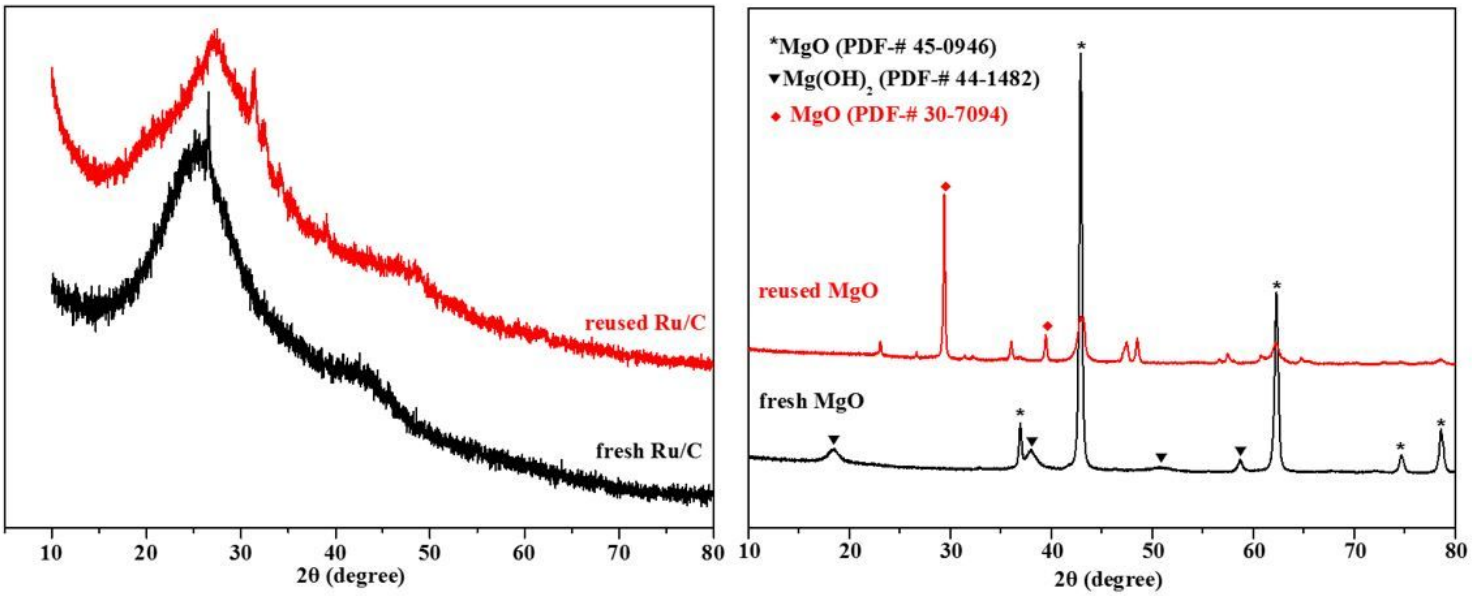

Figure 11

The XRD patterns of fresh and used Ru/C and MgO

Supplementary Files

This is a list of supplementary files associated with this preprint. Click to download.

- scheme1.jpg
- supportinginformation.docx